Lateglacial changes in river morphologies of northwestern Europe: An example of a smooth response to climate forcing (Cher River, France)

Anaëlle Vayssière, Mathieu Rué, Clément Recq, Philippe Gardère, Edit Thamó-Bozsó, Cyril Castanet, Clément Virmoux, Emmanuele Gautier

Lateglacial changes in river morphologies of northwestern Europe: An example of a smooth response to climate forcing (Cher River, France)

Anaëlle Vayssière [a,b,*], Mathieu Rué [c,d], Clément Recq [c], Philippe Gardère [e,f], Edit Thamó-Bozsó [g], Cyril Castanet [b,h], Clément Virmoux [b], Emmanuèle Gautier [a,b]

[a] Université Paris 1 Panthéon-Sorbonne, France
[b] Laboratoire de Géographie Physique, LGP CNRS-UMR 8591, 1 place Aristide Briand, Meudon, France
[c] Paléotime SARL, 6173 avenue Jean-Séraphin Achard-Picard, Villard-de-Lans, France
[d] Université Paul-Valéry Montpellier 3, Laboratoire Archéologie des Sociétés Méditerranéennes, ASM CNRS-UMR 5140, route de Mende, Montpellier, France
[e] INRAP, Centre de recherches archéologiques de Tours, 148 avenue André Maginot, Tours, France
[f] Laboratoire Cités, Territoires, Environnement et Sociétés, CITERES CNRS-UMR 7324, 33-35 allée Ferdinand de Lesseps, Tours, France
[g] Mining and Geological Survey of Hungary, Columbus street 17-23, Budapest, Hungary
[h] Université Paris 8 Vincennes-Saint-Denis, France

Geomorphology 342 (2019) 20–36
https://doi.org/10.1016/j.geomorph.2019.05.019
Postprint / author accepted manuscript

Abstract

Climate oscillations generally clearly recorded in current floodplains. The sites studied are located in the Cher River floodplain, which is one of the main tributaries of the Loire River. Several investigations have been conducted in the main valley, but few of them specifically focused on geomorphological evolutions of mediumsized catchments such as tributaries of the Loire River. Therefore, we examined this specific period through investigations recently conducted in the middle valley of the Cher River. This study aimed to (1) provide a geomorphological approach to fluvial adjustments during the Lateglacial from cases located in lowland areas of a mediumsized basin and (2) analyse the spatio-temporal variability of fluvial responses. Assessment of geomorphological trajectories of the two reaches studied highlights that fluvial metamorphosis occurring during the Lateglacial and early Holocene seems to be characterised by lateral readjustments and a low signal of morphological instability (shallow incision and aggradation processes, slow and progressive change in channel morphology). This observation is enhanced by the comparison with known geomorphological evolution patterns of adjacent basins. The intrinsic components of the Cher basin such as slope and valley width were considered as explanatory factors for the lack of morphogenetic processes. In addition, the geographical location of the reaches studied may also have led to a moderated expression of climate forcing. Indeed, the elevation as well as the north–south and east–west gradients may contribute to the low level of geomorphological adjustments in response to these climatic oscillations. This gradient could also have support this the fluvial response because of the weakly developed loess cover, which may have limited the fine sediment supply and the aggradation of the valley bottom.

Keywords: Floodplain Lateglacial, Fluvial metamorphosis, Palaeochannel, Cher River

1. Introduction

Transition from a cold to a milder climate and conversely during the Pleniglacial and Lateglacial periods is generally associated with several changes in fluvial dynamics. Climate-related changes in fluvial systems during the late Quaternary period have been the subject of an abundant literature aiming to propose evolution models (Houben, 2003; Mol et al., 2000; Vandenberghe, 2008, 2003, 1993; Vandenberghe et al., 1994). Fluvial geomorphological adjustments regarding climatic changes are described as a complex combination of processes involving climatic and non-climatic mechanisms. Previous studies conducted in northwestern Europe depict spatio-temporally variable responses during the Lateglacial (Houben, 2003; Mol et al., 2000; Vandenberghe et al., 1994).

Among these studies, several major issues can be considered as possible explanatory factors for geomorphological evolution, highlighting that fluvial systems are not steered solely by climate. Vandenberghe (2003) emphasised climate-derived factors such as permafrost and seasonally frozen soil, which control the permeability of slopes and enhance runoff during the melt period. He also stressed partially climate-dependent factors such as the vegetation cover. Indeed, slope susceptibility to erosion and sediment supply are impacted by vegetation type and distribution (Vandenberghe, 2003). Consequently, a short phase of morphologic instability (erosional or aggradation processes, changes in fluvial patterns) generally occurs because of the time lag of vegetation responses after a climatic change (precipitation and temperature) (Huisink, 2000; Vandenberghe, 1993). This emphasises the role played by climatic transitions in generating fluvial geomorphological instability. Spatio-temporal variability of fluvial system responses can also be explained by non-climatic factors referring to the intrinsic components of catchments (Houben, 2003; Kasse, 1998; Mol et al., 2000; Vandenberghe, 2003; Vandenberghe et al., 1994). It has been demonstrated, for example, that basin properties such as slope (Houben, 2003; Vandenberghe, 2003), floodplain width (Houben, 2003; Mol et al., 2000) and bedload grain size (Mol et al., 2000) could be considered as major explanatory factors of fluvial responses. Furthermore, the temporal trajectory of the river is controlled by threshold values that need to be exceeded to trigger any changes in the fluvial system (Schumm, 1979). These critical threshold values may explain the fluvial adjustments or lack of adjustment to climate changes (Mol et al., 2000; Vandenberghe, 2003; Vandenberghe and Woo, 2002). All these studies indicate that complexity characterises the relations between climate forcing and fluvial morphological adjustment. It underscores the need for approaches considering the entire catchment. Therefore, the multiplication of study cases and comparative approaches are needed to improve our knowledge of fluvial processes in response to climate-related stresses.

The transition from the Pleniglacial to the Lateglacial and from the Lateglacial to the early Holocene (ca. 14,700–11,500 cal. BP) is useful to study. It is generally well recorded in river valleys because it is the last glacial–interglacial transition (Vandenberghe, 2008). The Lateglacial consists of rapid climate changes classically sub-divided into a series of stadials referring to these oscillations. The knowledge of the response time of rivers to climatic stress can be improved by the study of this type of rapid transition. The Bölling-Allerød interstadial is the initial warm period of the Lateglacial occurring just before the Younger Dryas period (YD), an abrupt climate cooling (Rasmussen et al., 2014). Investigations conducted in northwestern Europe on continental pollen allowed the Middle Dryas (MD) to be recorded between Bölling and Allerød interstadials around 14 ky cal. BP (Leroyer et al., 2014; Magny et al., 2006). Then the transition to the early Holocene initiated milder climatic conditions that characterised the Holocene thermal maximum (Renssen et al., 2009).

The present study investigated several areas of the Cher River basin regarding spatio-temporal variability of morphological adjustments during the Lateglacial period. The Cher River is one of the main tributaries of the Loire River where several reaches of the valley were previously studied. These investigations were conducted in the upper basin (Cubizolle and Georges, 2002; Steinmann, 2015; Steinmann et al., 2017; Straffin et al., 1999; Straffin and Blum, 2002) and in the middle and low part of the valley (Carcaud et al., 2002; Carcaud, 2004; Castanet, 2008) as well as in a tributary (Loir River) (Piana et al., 2016, 2009) and in a very small subcatchment (Choisille River) (Morin et al., 2011) demonstrating how the Loire River evolved during the Lateglacial period. Nevertheless, few of these investigations specifically focused on geomorphological changes in medium-sized catchments such as the tributaries of the Loire River. Therefore, we examined this specific period provided by investigations recently conducted within the middle valleys of the Cher River. Middle valleys are generally known to enhance deposition processes because they are far from the torrential erosion that affects mountainous basins and also far from the coastal areas impacted by regressive erosion in response to sea-level changes (Richards, 2004). Moreover, the Cher basin is associated with a strategic location on the southern margins of northern Europe with periglacial heritages. Several collective investigations carried out on the northern part of the study areas show the persistence of the periglacial environment (ice wedge pseudomorphs, sand wedges, stripes, aeolian deposition) (Andrieux et al., 2016; Bertran et al., 2016).

Northern fluvial systems also provide a record of specific periglacial conditions during the YD such as aeolian deposits (Bohncke et al., 1993; Deschodt et al., 2012; Kasse et al., 2007; Vandenberghe et al., 1987), major phases of slope erosion (Antoine, 1997; Antoine et al., 2000, 2003, 2012; Pastre et al., 2000; Pastre et al., 2003) and cryoturbation of Bölling/Allerød deposits (Bohncke et al., 1993; Pastre et al., 2000; Pastre et al., 2003). Even if chronological data are generally scarce because they cover a short period and there is a lack of organic material suitable for radiocarbon dating, published investigations provide an abundant description of sedimentary facies deposited during the Lateglacial period. This scientific framework allows chronostratigraphic comparisons to be made considering previous studies and new insights contributed by the present study.

The aim of this study is to (1) provide a geomorphological approach to fluvial adjustments during the Lateglacial from cases located in lowland areas of a medium-sized basin and (2) analyse the spatio-temporal variability of fluvial responses. Considering the above-mentioned issues, the first step of our approach includes the synthesis of fluvial adjustments in two reaches studied during the Pleniglacial-Lateglacial-early Holocene. The second step, focused on spatio-temporal variability, aims to propose explanatory factors regarding spatial locations and morphologic parameters collected for each study area (location, catchment size, valley width, floodplain and river slope).

2. Regional setting

The Cher River is 368 km long and flows in a catchment covering 14,000 km^2. It is a tributary of the Loire River, which is the longest watercourse in France. The highest point of the Cher's course is 710 m and the lowest is 38 m at the junction with the Loire River. The upper basin is located in the Massif Central, which is mainly composed of crystalline rocks. Most of the basin consists of lowland areas situated in the South of the Paris sedimentary basin (Despriée et al., 2007; Larue, 1981; Voinchet et al., 2007).

The present study investigated two reaches: Thénioux and Noyerssur-Cher located in the middle valley of the Cher River (Fig. 1 and Fig. 2). Additional surveys were conducted at the Bigny site located upstream (Fig. 1). Despite an exhaustive investigation of the floodplain, no Lateglacial and early Holocene deposits were recognised. The alluvial area might be completely occupied by the late Holocene meander belt in the Bigny section (Vayssière, 2018; Vayssière et al., 2016). Nevertheless, surveys conducted downstream allow relevant fluvial archives to be identified in the Thénioux and Noyers-sur-Cher reaches that can help us to characterise fluvial adjustment in response to the latest climatic oscillations.

The Thénioux area is located a few kilometers downstream of Vierzon. The river drains an area covering 9070 km^2. The slope calculated from a longitudinal profile extracted from the DEM LiDAR (Digital Elevation Model - Light Detection And Ranging) is 0.695 $m.km^{-1}$ (Table 1). The geological bedrock corresponds to upper Cretaceous formations (Cenomanian sands and marl covered with Eocene flint clays) (Manivit et al., 1994). The Thénioux site is located immediately downstream of the confluence with the Yèvre and Arnon Rivers. The originality of this sector is the diversity of inherited landforms: straight wide palaeochannels and former sinuous channels have been identified through DEM analysis (Fig. 3).

The Noyers-sur-Cher site is located at the endpoint of the middle Cher River valley, defined by a meandering fluvial pattern. The river flows straight-line downstream until its confluence with the Loire River because of anthropogenic canalisation. The study area is located within the loop of the last meander on the convex bank of the river (at Le Busa). At this location, the floodplain mean slope is 0.51 $m.km^{-1}$.

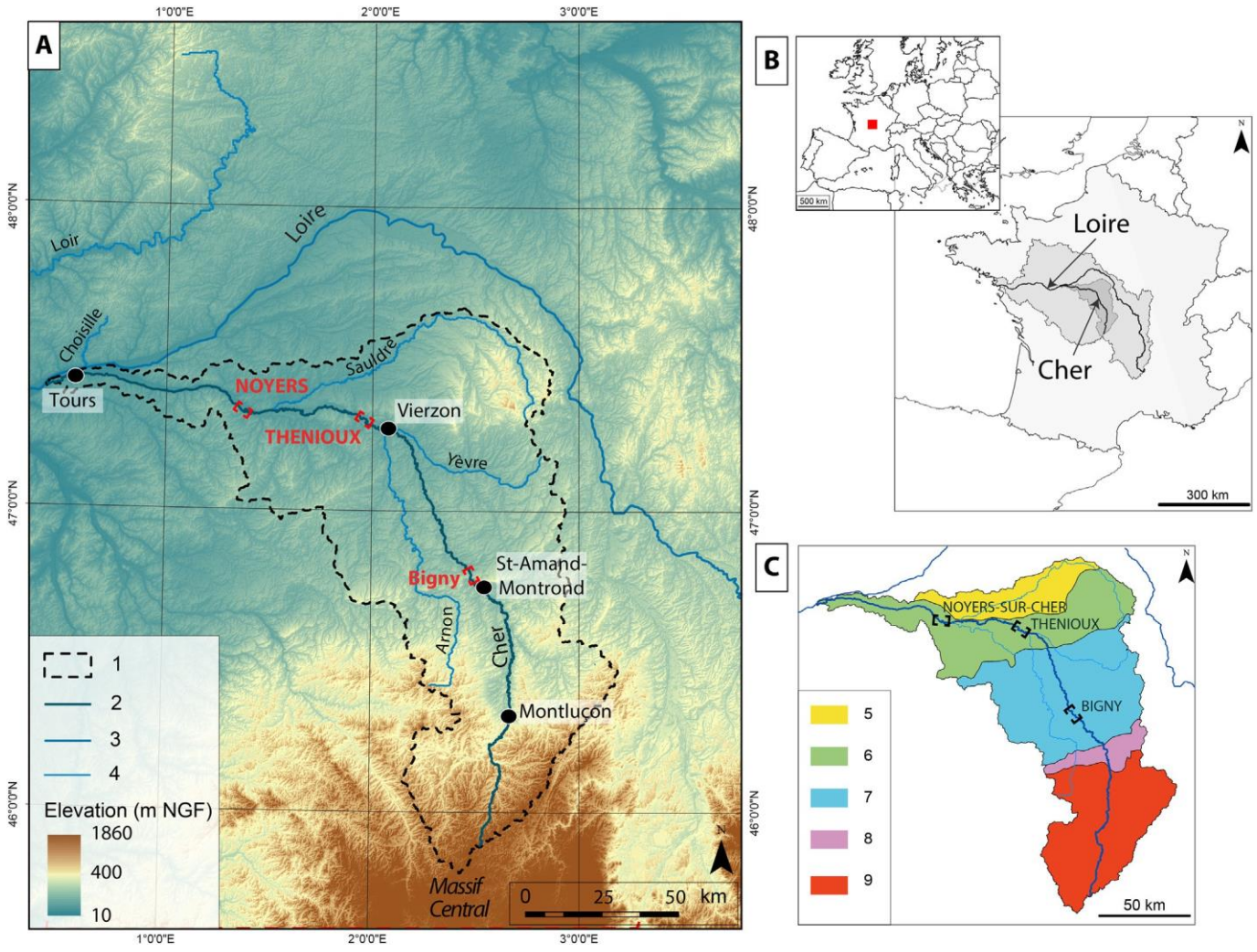

Fig. 1. A. Topographical map of the Cher River basin: 1. Cher River catchment; 2. the Loire River; 3. the Cher River; 4. secondary river. B. Location map. C. Main geological units; 5. PlioPleistocene sand; 6. Cretaceous limestone; 7. Jurassic limestone; 8. Triassic limestone; 9. Plutonic and magmatic rock (Massif Central).

3. Methodological approach

The topography of the alluvial plain was analysed using LiDAR DEM. Such data sets allow postglacial fluvial patterns to be highlighted through topographic variations. Boreholes and an electrical imaging survey helped to estimate the geometry of former channels. Cores collected in palaeochannels and excavation surveys provided samples suitable for radiocarbon and OSL (Optically Simulated Luminescence) dating.

3.1. DEM LiDAR analyses

DEM LIDAR provides an accurate topographic data set suitable for identifying former fluvial landforms such as abandoned channels and bars. Indeed, in a geomorphological context with a low-contrast topography such as a floodplain, this tool enables one to discern the shapes of the relief very precisely (Notebaert et al., 2009). The LiDAR data were acquired in the Cher valley between 2009 and 2011 and were provided by the DREAL (Direction régionale de l'environnement, de l'aménagement et du logement; Regional Institute of the Environment, Development and Housing) in the form of a pixel matrix. The whole surface of the floodplain is covered by 1 × 1-km geo-referenced tiles. First, the tiles corresponding to the areas studied were merged using GIS software (ArcGIS 10.4). A second type of treatment consists in correcting the longitudinal inclination of the valley floor. The method consists in subtracting a DEM whose inclination corresponds to the slope of the valley from the original DEM. Following the example of the survey conducted in the Burgundian Loire valley (Steinmann, 2015; Steinmann et al., 2017), we used the average slope of the water line to generate the inclined DEM. These data were extracted from the 2009 and 2011 LiDAR DEMs by assuming that the pixels adjacent to the river bed correspond to the elevation of the water line. Therefore, different reference points were placed preferring areas of convex point bars and avoiding areas where the banks are steep. From each of these points, a contour perpendicular to the axis of the valley was derived to generate the inclined DEM. By displaying the relative elevation, inherited landforms were easily identified, digitalised and mapped.

3.2. Floodplain filling architecture

To take into account the lateral variability of alluvial filling, extended cross-sections of valley bottom were produced including boreholes, outcrops and geophysical surveys. Lithofacies were determined according to the Miall terminology (Miall, 1996). The deposits were sequenced in stratigraphic units (SU) based on texture, structure and color.

Sixty-seven mechanical and manual boreholes were drilled in the Thénioux site. A documentary research provided additional boreholes from previously reported surveys. Nineteen additional stratigraphic logs were supplied by the BRGM (Bureau des Recherches Géologiques et Minières; Mining and Geological Research Institute) and twenty-six logs by the CEREMA Centre-Normandie (Centre d'études et d'expertise sur les risques, l'environnement, la mobilité et l'aménagement, Centre for Studies and Expertise on Risks, Environment, Mobility and Development). At Noyers-sur-Cher, archaeological trenches, created before the extension of a quarry in a rescue archaeology context, on a total surface of about 24,000 m^2, enabled the study of two long continuous crosssections (TR1 and TR2).

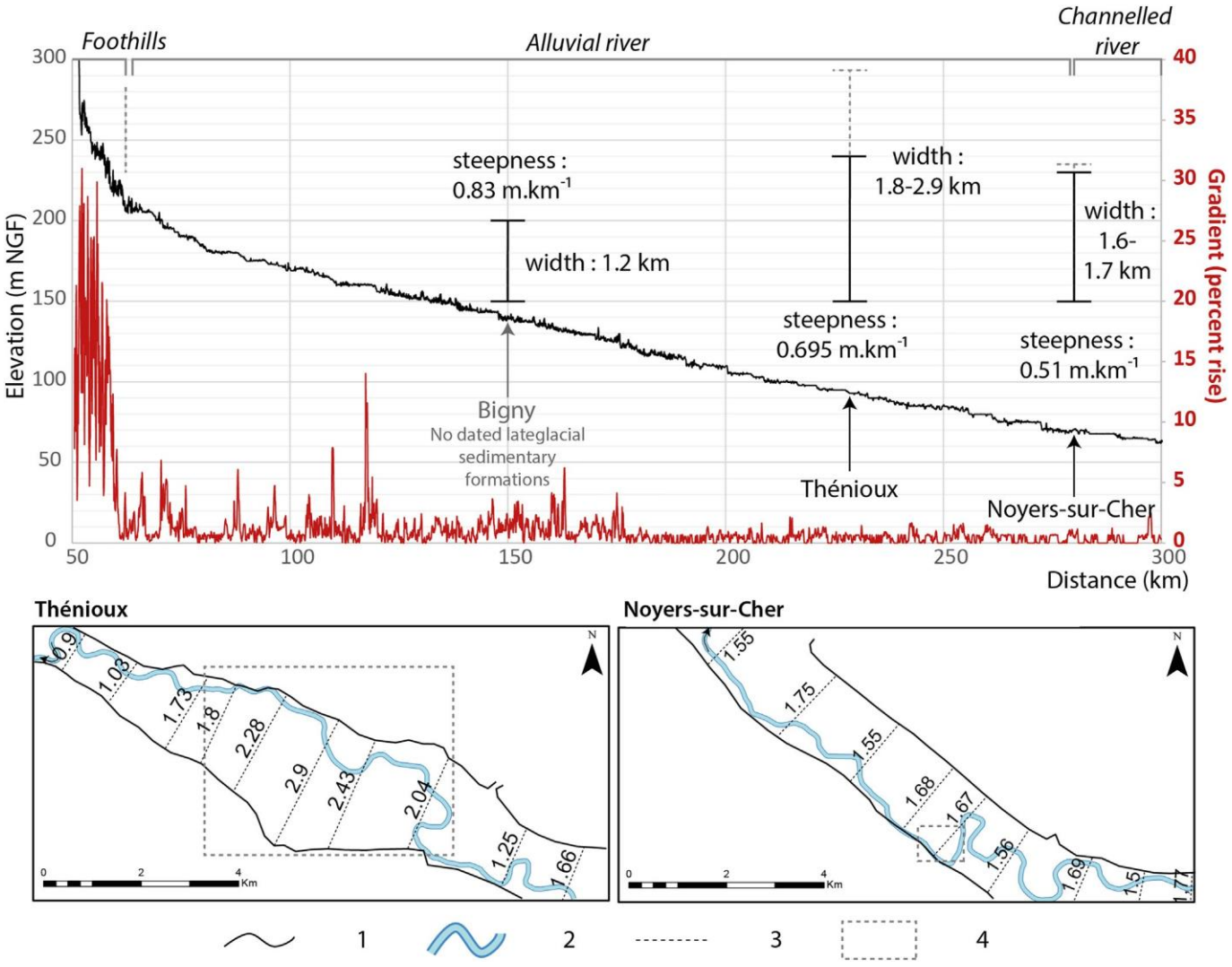

Fig. 2. Physiographic properties and location of each reach studied. 1. boundary of valley floor; 2. river; 3. valley floor width survey; 4. reaches studied. The boundaries of the valley floor were defined according the geological map(1/50000) provided bythe BRGM (Bureau des Recherches Géologiques et Minières). The long profile was extracted from DEM (Digital Elevation Model) data provided by IGN (Institut Géographique National) with an accuracy of one measurement every 75 m.

Study area	Catchment size (km²)	Valley floor width (km)	Current mean discharge ($m^3.s^{-1}$)	Floodplain slope ($m.km^{-1}$)	River slope ($m.km^{-1}$)	Distance from the source (km)	Current fluvial pattern	Coordinates (WGS 84)
Thénioux	9070	1.8-2.9	61.9	0.695	0.46	228	Sinuous to meandering	Long: E 1.894; Lat: N 47.252
Noyers-sur-Cher	11540	1.6-1.7	74.5	0.51	0.4	280.5	Sinuous to meandering	Long: E 1.23; Lat: N 47.16

Table 1
Main hydro-sedimentary characteristic of studied reaches.

A geophysical survey was also conducted to identify palaeochannels and other former fluvial landforms (bars, islands, floodplain deposits). Electrical resistivity tomography (ERT) depicts the distribution of the subsoil electrical resistivity value (Loke, 1999; Marescot, 2006). The electrical resistivity of the subsoil (ρ expressed in ohm·m) refers to the ability of the sediment and bedrock to conduct electrical power. This property varies according to different parameters such as porosity, degree of water saturation, dissolved salt content and to a smaller extend temperature. It is a suitable tool to assess the dimension of palaeochannels. Indeed, palaeochannel filling generally consists of low-resistivity sediment (silt and clay). Two-dimensional 766-m-long electrical resistivity tomography was carried out at Thénioux using an ABEM Terrameter LS sensor. The protocol used for this survey corresponds to the Wenner-Schlumberger array with electrodes spaced 2 m apart. A planimetric geophysical survey measuring electric resistivity was conducted at Noyers-sur-Cher by the company Geocarta using the automatic resistivity profiling (ARP) method (Dabas, 2009; Genelle et al., 2014). ARP uses a patented multi-electrode device that is connected to wheel-based electrodes that roll over the ground surface. The spacing of the dipoles integrates increasing volumes of soil (0–0.5 m, 0.5–1.0 m and 1.0–1.7 m). The ARP measurements were taken over 0.116 km^2. Data were acquired every 0.1 m along parallel survey lines spaced 6 m apart. The data processing involved spline interpolation on a 2-m regular mesh.

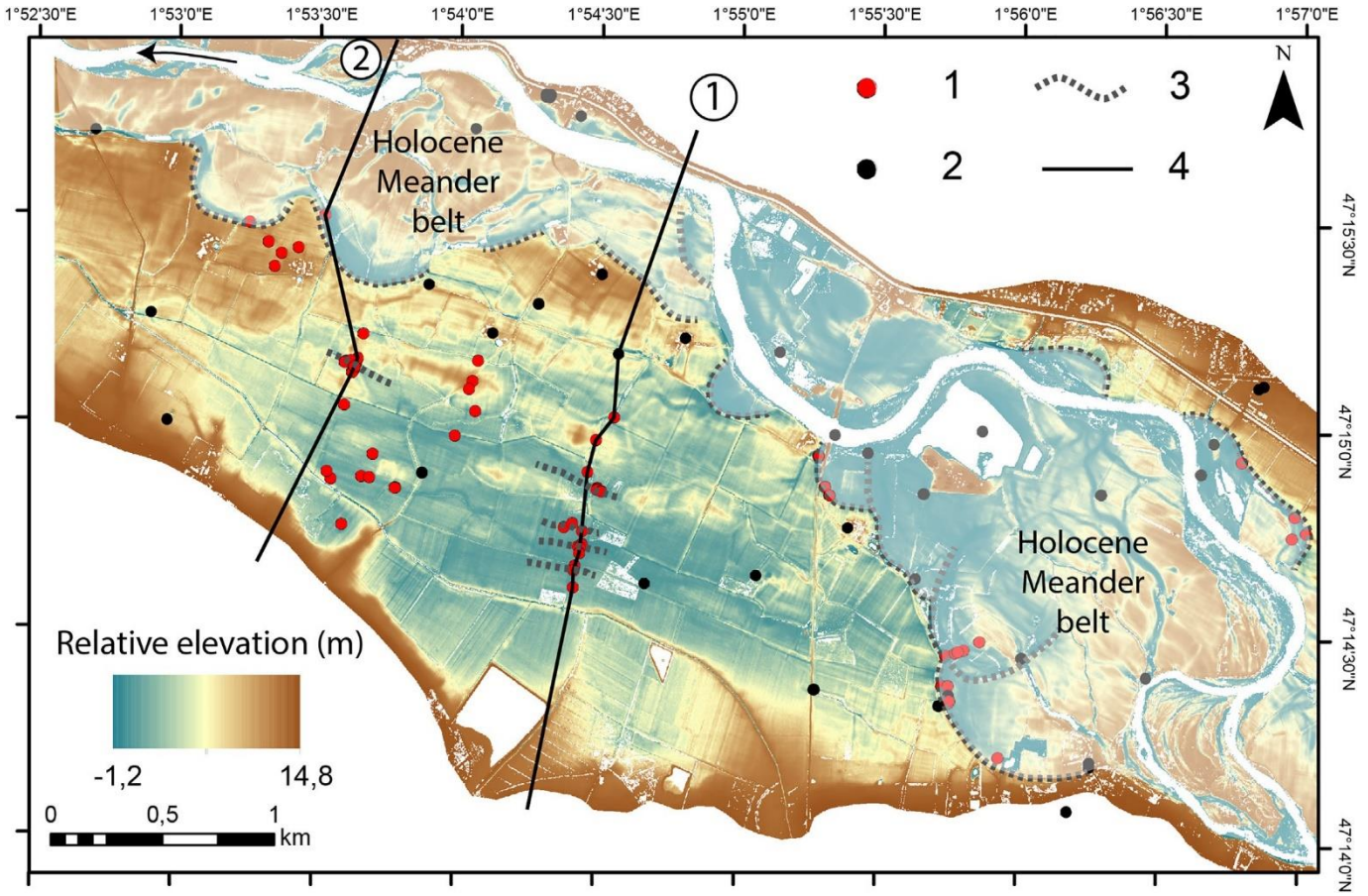

Fig. 3. Topographical and borehole surveys conducted at Thénioux. 1. borehole from fieldwork; 2. borehole from documentary research; 3. palaeochannel; 4. synthetic cross-section.

3.3. Palaeochannel filling analyses

The core TRG7 from a palaeochannel of the Thénioux site, abandoned at least since the Allerød period, was studied in order to reconstruct the environmental conditions following the cutoff. Grain-size was analysed on 44 samples cleared from the organic matter by laser diffraction with a Beckmann-Coulter LS230. Grain size indices were calculated using the GRADISTAT 8.0 program (Blott and Pye, 2001). The grain-size scale adopted in this study was built according to Konert and Vandenberghe (1997); Udden (1914); Wentworth (1922). These analyses help to characterise the sedimentary facies. Qualitative observations also were conducted through a preliminary micromorphological approach and the fraction coarser than 50 µm was observed with binoculars.

3.4. Chronology of fluvial deposits

The location of palaeochannels in the valley bottom enables the reconstruction of the relative chronology of the cutoffs. The age of fluvial deposits is based on 16 radiocarbon AMS dates of organic material sampled within the palaeochannel (Table 2) through boreholes or excavation surveys. Radiocarbon ages were calibrated using the OxCal v4.3.2 (Bronk Ramsey, 2009) according to the IntCal13 atmospheric curve (Reimer et al., 2013). Basal parts of abandoned channel filling were dated to provide the approximate age of the cutoff.

Trench surveys carried out at Noyers-sur-Cher allowed samples for OSL dating to be collected. Three samples were analysed. Samples for luminescence measurements were prepared in a dark room under subdued red light conditions. The few sunlight-contaminated centimetres of the sediments were removed at the two ends of the sampling tubes and were not used for dating. During sample preparation sieving, 20% H_2O_2, 10% HCl, sodium polytungstate (SPT) and 40% HF for 60 min were used according to Aitken (1998, 1985). One hundred- to 160-µm quartz grains were mounted on stainless-steel discs in a 5-mmdiameter monolayer using silicone spray.

OSL measurements were performed using Risø TL/OSL DA-15C/D and DA-20 readers with a calibrated 90Sr/90Y beta source. Luminescence was stimulated by blue-light-emitting diodes (λ = 470 ± 20 nm) for 40 s at 125 °C. The resulting OSL signals were collected through a UV filter (Hoya U-340). The single-aliquot regenerative-dose (SAR) protocol was applied (Wintle and Murray, 2006), and in addition to equivalent dose measurements, different tests were performed. Infrared tests indicated that 97–100% of the measured aliquots were pure quartz. Depending on the results of the preheat plateau tests and thermal transfer tests, 260 °C preheat temperature was applied in the case of samples 132.1 and 132.2, and 240 °C for sample 163.1; cut heat was 200 °C.

Study area	ID	Location	Sample code	Material	Depth below the current surface (m)	Elevation (m NGF)	Radiocarbon age (BP)	Intervalle confidence	Calibrated date, 2 sigma (95.4%) (cal. BP)
Thénioux	Th1	TRG6, infilling	Beta-441217	Organic sediment	1,89-1,9	89,2-89,21	11960	50	14004-13702 and 13678-13620
Thénioux	Th2	TRG6, base of the channel infilling	Beta-441218	Organic sediment	2,76-2,77	88,84-88,85	12600	50	15179- 14694
Thénioux	Th3	TRG7, base of the channel infilling	Poz-75170	Organic sediment	2,15-2,16	87,74-87,75	11890	60	13940-13553
Thénioux	Th4	TRG7, base of SU3	Poz-77943	Organic sediment	2-2,014	87,885-87,9	10690	50	12718-12569
Thénioux	Th5	TRG7, base of SU2	Poz-78014	Organic sediment	1,81-1,82	88,08-88,1	9070	50	10378-10169
Thénioux	Th6	TRG7, middle of SU2	Poz-77942	Organic sediment	1,445-1,47	88,43-88,45	9520	50	11090-10610
Thénioux	Th7	TRG7, base of SU1	Poz-78013	Organic sediment	0,84-0,86	89,04-89,06	8160	50	9262-9009
Thénioux	Th8	TRG5, base of the infilling	Beta-441215	Organic sediment	2-2,01	87,08-87,09	5000	30	5888-5819 and 5762-5652
Thénioux	Th9	TRG4, base of the infilling	Beta - 441214	Organic sediment	2,68-2,7	86,16-86,18	3000	30	3326-3298 and 3253-3076
Thénioux	Th10	TRG4, infilling	Beta - 441213	Organic sediment	1,87-1,88	86,98-86-99	2600	30	2773-2715
Noyers-sur-Cher	N1	section CP5, CH1 infilling	Poz-90001	Bone	0,98	67,45	225	30	310-(19)
Noyers-sur-Cher	N2	section CP1.7, PR9, SU3a	Poz-90234	Organic sediment	0,89	67,44	4960	50	5859-5829 and 5752-5601
Noyers-sur-Cher	N3	neolithic pit ST2 opening at the base of SU2	Poz-90004	Wood charcoal	0,68	67,66	4710	40	5583-5507, 5489-5439 and 5421-5322
Noyers-sur-Cher	N4	archaeological layer at the base of SU2 (square F34)	Poz-90003	Wood charcoal	0,56	67,82	2785	30	2957-2795
Noyers-sur-Cher	N5	archaeological layer at the base of SU2 (square F39)	Poz-90002	Wood charcoal	0,42	67,98	3360	30	3692-3660, 3650-3557 and 3534-3496
Noyers-sur-Cher	N6	archaeological layer at the base of SU2 (square F39)	Poz-90005	Wood charcoal	0,44	68,00	3360	35	3694-3658, 3652-3650 and 3536-3484

Table 2
AMS-radiocarbon dates from the Cher River valley (calibration with OxCal v4.3.2 (Bronk Ramsey, 2009)) according to the IntCal13 atmospheric curve (Reimer et al., 2013).

Dose recovery ratios, recuperation values and recycling ratios were satisfactory. The growth curves indicated that the samples were not saturated. Age calculation was based on the mean equivalent dose (D_e) value of 26 aliquots in the case of samples 132.1- and 132.2, which have symmetric D_e distributions. But the measured 69 D_e of sample 163.1 showed an asymmetric distribution; therefore, the central age model (CAM) and minimum age model (MAM) of Galbraith et al. (1999) and the finite mixture model according to Galbraith and Green (1990) were also applied. Among them principally the age based on MAM reflects the best stratigraphic order of the sediment layer of sample 163.1.

Dose rates of the sediments were calculated based on laboratory highresolution gamma spectrometry measurement (Canberra GC3020) of bulk samples using the conversion factors of Adamiec and Aitken (1998). Cosmic dose rates were calculated according to Prescott and Hutton (1994); Prescott and Stephan (1982). The water content of the sediments during the time span of burial was estimated about 24% (samples 132.1 and 163.1) and 13% (sample 132.2), which represents the medium water content between the measured recent and saturated water content values. Since the three samples were close to the current water table (and even inside the water table in winter), the results obtained with a saturated water content are preferred (Table 3).

Location	Sample code	Material	Depth below the current surface (m)	Elevation (m NGF)	Equivalent dose (Gy)	Dose rate (Gy/ky)	Water content (%)	Age model	OSL age (ky BP)
trench TR1, section G16, SU3s	MBFSZ 132.1	quartz	0,75	68,65	30,10 ± 0,94	3,21 ± 0,23	22,7 (recent)	Mean	9,4 ± 0,8
						3,19 ± 0,23	23,7 (medium)		9,4 ± 0,8
						3,16 ± 0,22	24,6 (saturated)		**9,5 ± 0,8**
trench TR1, section G19, SU5	MBFSZ 132.2	quartz	1,20	67,55	45,29 ± 0,64	3,65 ± 0,28	4,0 (recent)	Mean	12,4 ± 1,0
						3,32 ± 0,25	13,2 (medium)		13,6 ± 1,1
						3,05 ± 0,23	22,4 (saturated)		**14,8 ± 1,2**
trench TR2, section CP1.7, PR4, SU4	MBFSZ 163.1	quartz	1,18	67,16	51,27 ± 0,94	3,50 ± 0,25	16,2 (recent)	Mean	14,7 ± 1,1
						3,26 ± 0,23	24,1 (medium)		15,7 ± 1,2
						3,05 ± 0,21	32,1 (saturated)		16,8 ± 1,3
trench TR2, section CP1.7, PR4, SU4	MBFSZ 163.1	quartz	1,18	67,16	42,36 ± 1,46	3,50 ± 0,25	16,2 (recent)	Minimum	12,1 ± 1,0
						3,26 ± 0,23	24,1 (medium)		13,0 ± 1,1
						3,05 ± 0,21	32,1 (saturated)		**13,9 ± 1,1**

Table 3
Optically stimulated luminescence (OSL) measurements from Noyers-sur-Cher.

4. Fluvial adjustments in two study areas during Pleniglacial Lateglacial and Lateglacial-early Holocene transitions

4.1. Upstream reach: Thénioux

4.1.1. Age and locations of Lateglacial fluvial archives

Extended cross-sections coupled with LiDAR DEM analyses allowed Lateglacial inherited fluvial landforms to be identified (Fig. 3 and Fig. 4). They are located in the floodplain and cover a large portion of the alluvial area. The other part of the floodplain corresponds to a Holocene meander belt. The older Holocene palaeomeander recognised at Thénioux (TRG5) was cut just before 5888–5652 cal. BP (sample Th8) (Vayssière, 2018). According to topographical and borehole surveys, Lateglacial inherited landforms consist of elongated shape slightly elevated areas - which we will refer to as “montilles”-separated by straight palaeochannels abandoned during Bölling and Allerød interstadials. No significant difference in relative elevation between the Holocene meander belt and Lateglacial deposits was revealed in the topographical analyses (Fig. 3 and Fig. 4).

Two areas (focus 1 and focus 2) were studied in details in order to characterise precisely the sedimentary architecture of Lateglacial deposits (Fig. 4).

The **first focus** is based on ten boreholes and the 766-m-long electrical resistivity survey (Fig. 5). The boreholes L9 and L10 denote that the top of substratum consists of compact dark clay characterised by low resistivity values (between 0 and 55 Ω·m). Geophysical survey indicates that the top of this bedrock has a sloping shape inclined toward the SW (Fig. 5).

Five main sedimentary units were distinguished:

- Coarse alluvia composed of sands, gravels and pebbles (GB-Gcm, GBGp) and characterised by high resistivity values (80–160 Ω·m). There were observed at the base of the floodplain sedimentary formation at the contact with the bedrock (base of the boreholes L5, L7 and L8). There were interpreted as a former alluvial sedimentary sheet incised by the paleochannels of the Lateglacial.

- Composite layer constituted of silty matrix-supported sands and gravels (GB-Gmm, CS-Gmm, CS-Sm) also characterised by high resistivity values (80–160 Ω·m). It was recognised through the boreholes L5, L7 and L8 covering the coarse basal unit. It was also identified overlying the bedrock at the base of the borehole L9. It was interpreted as a transitional layer.
- Massive or silty matrix-supported sandy alluvia (CS-Sm, CSGmm, GB-Gcm; GB-Gmm), characterised by medium resistivity values (50–80 Ω·m) and interpreted as over bank sandy deposits or former bedload. They were mainly observed at the base of the silty clayey fillings of palaeochannels (boreholes L5, L6, TRG6, L7, L8 and L9)
- Sandy silts (CH-Fl, FF-Fl) that probably result from the vertical migration of fine particles to the bottom. Resistivity values ranges approximatively from 20 to 55 Ω·m. They were observed between the former bedload and the silty clayey fillings of the palaeochannels (boreholes L1, L2, L3, L5, L6 and L7) and between palaeochannels structures (boreholes L4 and L8).
- Silty clays constituting the filling of the palaeochannels (CH-Fsm) associated with low resistivity values (0–20 Ω·m). They were identified through the boreholes L1, L2, L3, L5, and L7. These deposits sometimes contain organic remains (TRG6) or ferruginous and carbonate concretions. Silty deposits are also systematically observed at the top of the floodplain formations. These are overbank deposits formed in a terrestrial floodplain context (FF-Fsm, FF-Fl).

These morphostratigraphical information enable to identify several architectural elements. The borehole L9 allows us to specify the lithological composition of the “montille” M1. The substratum is located at a depth of 4 m and is covered by a 1.1 m thick sedimentary unit composed of medium and coarse sands grey to brown (Cs-Sm). This unit is overlain by 2.2 m thick silty matrix-supported sands and gravels (CsGmm) probably due to the vertical migration of fine particles. This formation is covered by 0.7 m thick slightly sandy silts (FF-Fl) probably resulting of the alluviation of the floodplain. Two wide palaeochannels (T1 and T2) are characterised by a sandy filling with resistivity values between 20 and 55 Ω·m. The palaeochannels structures lay on the sheet of gravels and pebbles, as shown by boreholes L5, L7 and L8 and by high resistivity values (80–160 Ω·m). The architecture of the palaeochannels appears to be nested. Smaller palaeochannels (T11, T21, T22 and T23) are characterised by silty clay filling whose resistivity values range from 0 to 20 Ω·m. The filling of the palaeochannel T21 (borehole TRG6) provided organic material suitable for radiocarbon dating. Two chronological markers denoted that palaeochannel T21 started to fill around 15,179–14,674 cal. BP (beginning of the Bølling; sample Th2). The filling process continued until 14,004–13,620 cal. BP (sample Th1) and later.

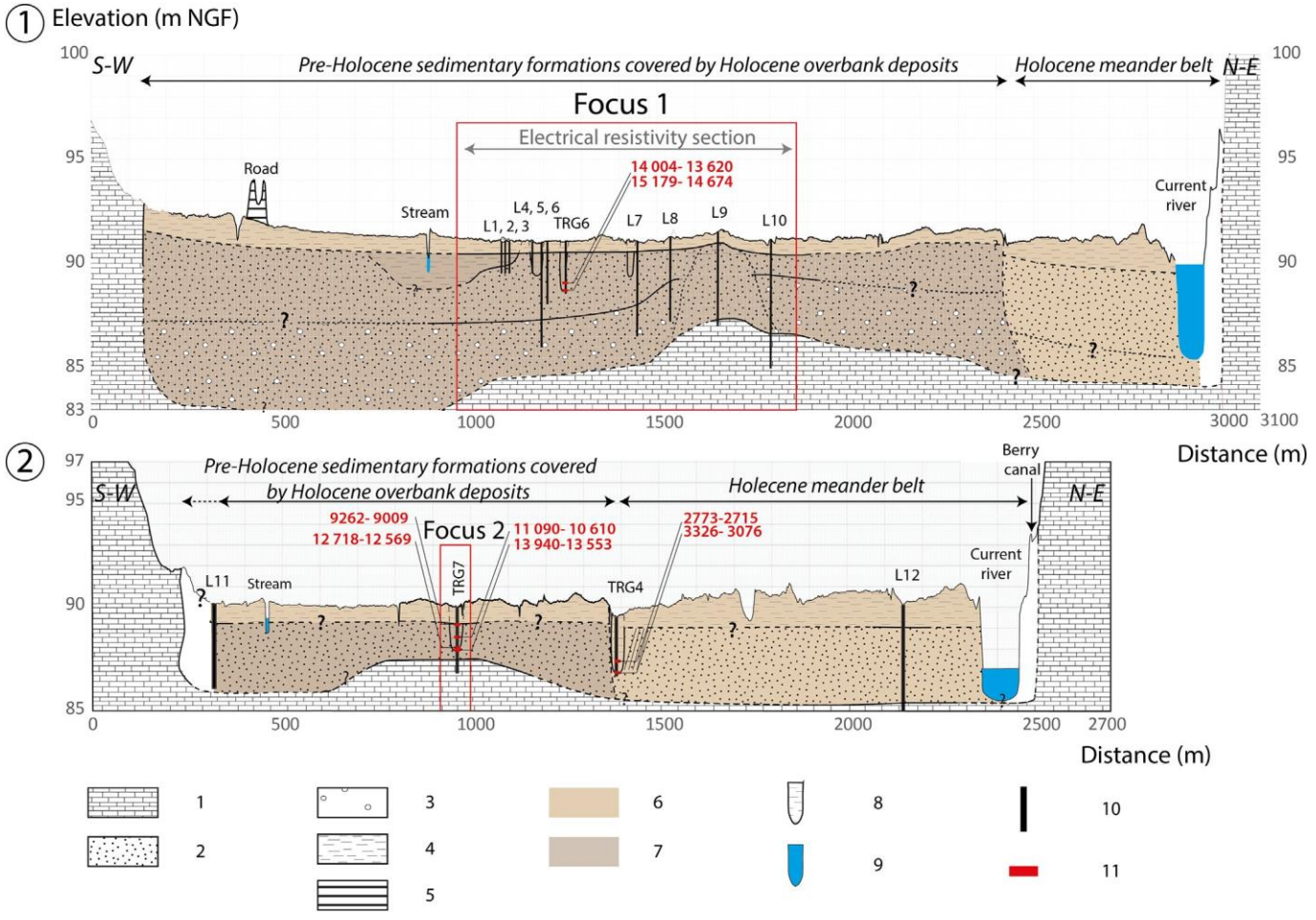

Fig. 4. Synthetic cross-sections of the floodplain filling at Thénioux. A. Cross-section 1; B. Cross-section 2. 1. geological substratum (bedrock); 2. coarse alluvia (sands and gravels); 3. coarse alluvia (sand gravels and pebbles); 4. fine alluvia (clay and silt); 5. anthropogenic backfill; 6. post-glacial deposition (Holocene); 7. Lateglacial and older deposition; 8. palaeochannels; 9. current stream and river; 10. borehole; 11. radiocarbon age.

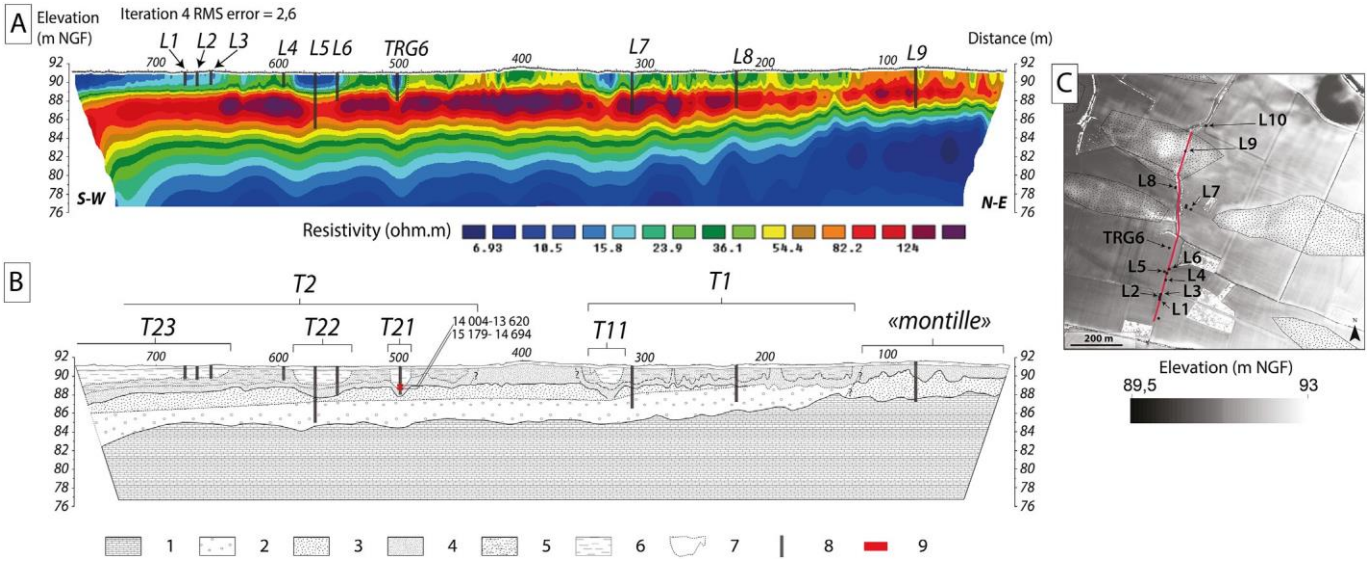

Fig. 5. Focus 1: Electrical resistivity survey and proposed interpretation. A. Electrical resistivity survey in fluvial sedimentary formations and their bedrock; B. proposal for sedimentary architecture; C. location of electrical resistivity survey: 1. geological substratum (bedrock); 2. coarse alluvia composed of sands, gravels and pebbles (GB-Gcm, GB-Gp); 3. transitional layer composed of sandy and gravel silty matrix-supported (GB-Gmm, CS-Gmm, CS-Sm); 4. sandy alluvia (CS-Sm, CS-Gmm, GB-Gcm, GB-Gmm); 5. sandy silt (CH-Fl, FF-Fl); 6. silty clay (CH-Fsm, FF-Fsm, FF-Fl); 7. proposal for palaeochannel boundary; 8. borehole; 9. radiocarbon age.

This assemblage of palaeochannels probably corresponds to a multiphase sedimentary formation composed of two wide palaeochannels (T1 and T2) that could have been inherited from former braided, laterally active reaches. Within these large palaeochannels, smaller flow structures filled with silty clay deposits were interpreted as subsequent reactivations. The bottoms of the filling of the palaeochannels have almost the same elevation. However, there is a slight difference of b1 m between the bottom of the filling of TRG6 and those of T22. It could be interpreted as a very shallow incision but the signal is very weak and the indicator is not completely reliable.

The **second focus** is based on eleven boreholes drilled very close to each other in order to characterise the sedimentary architecture of the palaeochannel TRG7 precisely (Fig. 6). The palaeochannel filling seems to be multi-phased, indicating several phases of reactivation. In the centre of the palaeochannel, silty clayey formations were deposited during the last filling phase. The lateral extremities of the palaeochannel filling are characterised by more sandy deposits probably due to an older phase of filling or bank collapsing (Fig. 6). Five radiocarbon ages show that the palaeochannel started to be filled not later than 13,940–13,553 cal. BP (Allerød period; sample Th3). The filling process continued during YD (12718–12,569 cal. BP; sample Th4) and early Holocene (11090–10,610 cal. BP and 9262–9009 cal. BP; sample Th6 and Th7, respectively). The age 10,378–10,169 cal BP (sample Th5) has not been exploited because of a stratigraphical inversion and because the carbon content was too low (0.5 mgC). The base unit (SU 5), lying on the bedrock, was composed of sands and gravels (GB-Gcm/Gmm). It was interpreted as the persistence of dynamic flows able to transport coarse material. Overlying deposition (SU4, SU3, SU2 and SU1) consisted of silty clay denoting a less energetic depositional environment (CH/FF-Fsm). SU4 was composed of dark grey organic silty clay (CH-Fsm) interpreted as the signal of fluvio-palustrine deposition taking place in a palaeochannel converted into a pond. The base and the top of SU4 (samples Th3 and Th4) were dated around 13,940–13,553 cal. BP (Allerød) and 12,718–12,569 cal. BP (Younger Dryas). From SU3 up to the top of the core, lithogenic deposition characterised by alluvial silt and sands and micritic concentrations was interpreted as the transition toward a terrestrial environment. It is likely that SU3 (CH-Fsm) deposition would take place in a hydromorphic environment that was probably seasonally dewatered. SU2 and SU1 were mainly composed of massive dark grey silty clay (CH/FFFsm) -containing shells and pedogenetic secondary carbonated concretions. This deposition was attributed to Preboreal and Boreal periods according to chronological markers located 0.84 m (9262–9009 cal. BP; Th7) and 1.445 m deep (11090–10,610 cal. BP; Th6). The thickness of SU1 represents the deposition balance of the last 9262–9009 years. As a consequence, the sediment rate is much lower. The accurate litho-stratigraphical approach conducted on core TRG7 highlights the relative continuity of the deposition process recorded within the palaeochannel. Indeed, there was no obvious change in sedimentation facies in spite of climatic oscillations such as Allerød/YD and YD/early Holocene transitions.

4.1.2. Synthesis of adjustment of fluvial morphology during the Lateglacial

The lateral boundaries of Lateglacial deposits are defined by the Holocene meander belt. Comparison of Weichselian and Holocene palaeochannels through the DEM LiDAR (Fig. 3) and the boreholes (Fig. 4, Fig. 5 and Fig. 6) highlights a change in the fluvial pattern and a shift of the river bed toward the northeastern part of the valley. The fluvial pattern evolved from straight channels during the Lateglacial period to a sinuous or meandering path during the second half of the Holocene. More precisely, floodplain fluvial archives of the Thénioux reach identified three main steps.

(1) Older chronological markers consisted of palaeochannel filling associated with Bölling and Allerød interstadials. No floodplain deposit was directly attributed to the Pleniglacial or Older Dryas period. Before the Bölling/Allerød interstadials, flows were probably concentrated in former braided reaches without strong channel entrenchment. The “montilles” were interpreted as a topography inherited from former point bars or islands formed during the late Pleniglacial in the context of the braided system. It is likely that they were stabilised during the Lateglacial through the concentration of flows in stable reaches. Small palaeochannels suggest side arms associated with a main channel. Hence, during the early Lateglacial, the fluvial pattern could have been composed of at least two straight channels including one main arm and lateral

channel(s). It might correspond to a “transitional system” between braided multichannels pattern and a meandering single channel as described by Bohncke et al. (1995); Huisink (1997); Kasse et al. (1995); Vandenberghe et al. (1994). During the Bölling and Allerød interstadials, abandoned channels were filled with organic silt and peaty depositions. The persistence of this fluvial pattern is attested at least up to 13,940–13,553 cal. BP (Allerød period).

(2) Fluvial archives attributed to YD and early Holocene consisted of lithogenic silty palaeochannel filling affected by dewatering and pedogenetic processes. Our observations carried out on these floodplain deposits did not find significant changes in sedimentation processes in response to climatic oscillations. No fluvial active landform such as palaeochannels, former bars and islands were attributed to this period. Hence, the channel morphology is unknown, but it is likely that the fluvial pattern composed of one straight main arm and lateral channel(s) persisted during YD.

(3) Signals of the transition to a meandering pattern were recorded around 5888–5652 cal. BP at the latest. Despite an extensive survey, few deposits were attributed to the first half of the Holocene. Thus, two hypotheses can be raised. It can be interpreted as the reworking of sedimentary formations through lateral migrations of Holocene meanders. It can also be suggested that a low level of aggradation of the floodplain and lateral stability of the channels may have characterised the fluvial system during this period. An anabranching fluvial pattern could explain why recorded aggradation appears to be very low after the Allerød period. Indeed, according to the model proposed by Nanson and Knighton (1996), a cohesive sediment anastomosing river (Type 1b) could correspond to a stable sinuous multi-channel pattern associated with few bedload deposits. This fluvial pattern could have been predominant during the first half of the Holocene. This hypothesis is reinforced because no active fluvial landform was attributed to the period from Allerød up to ca 6000 cal. BP, implying moderate mobility of the channel. This type of fluvial pattern could have been promoted by the heavily forested floodplain context during the Atlantic (ca 8500–6500 cal. BP), as shown by vegetation reconstruction in the low valley of the Loire River (Cyprien et al., 2004; Visset et al., 2005). Similar river patterns are described in most of the low-energy rivers of Western Europe in a pre-deforestation context (Brown et al., 2018; Harwood and Brown, 1993; Lespez et al., 2015).

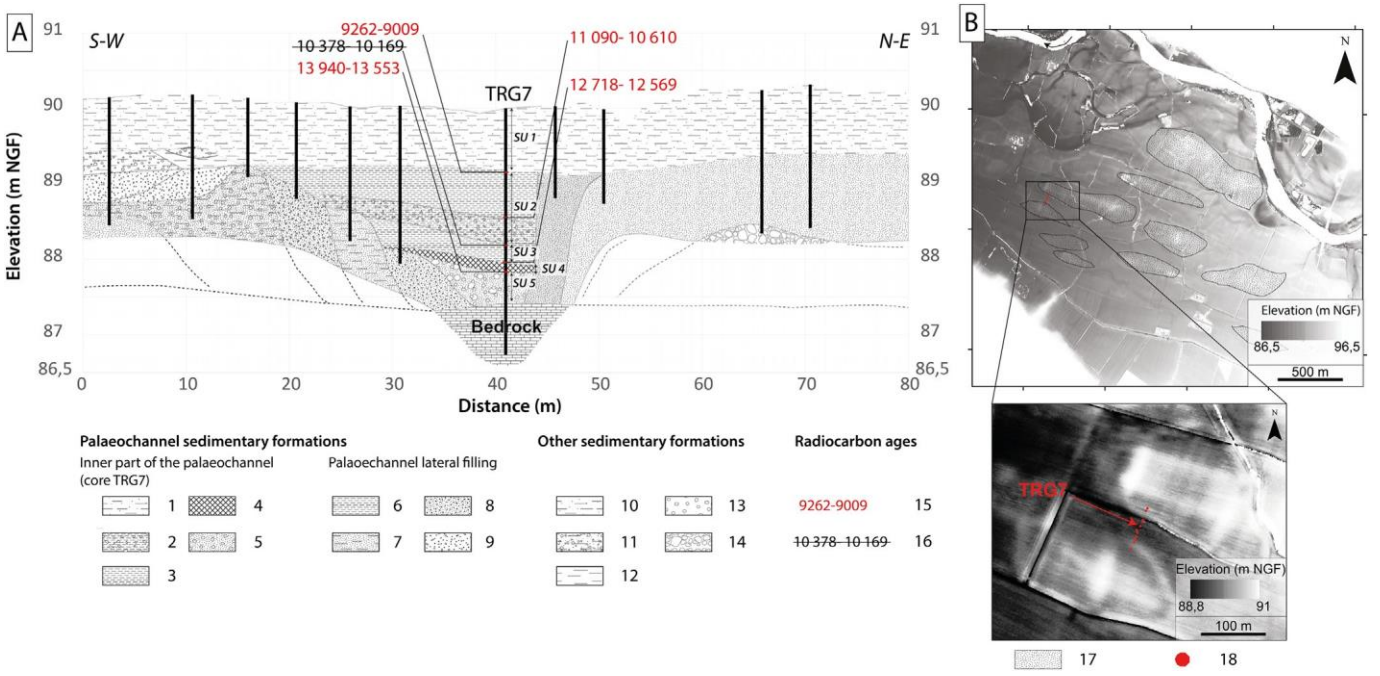

Fig. 6. Focus 2: sedimentary architecture of a Lateglacial palaeochannel at Thénioux. A. Proposal for sedimentary architecture of a palaeochannel filling and adjacent “montilles”; 1. dark grey silty clay with white concretions and iron nodules (CH-Fsm); 2. white concretions and shell silty matrix-supported, iron nodules (CH-Fsm); 3. bluish silty clay, darker bedding, iron nodules at the top of the layer (CH-Fl); 4.organic silt, organic remains(CH-Fsm/P); 5. orange sands and gravels (GB-Gcm/Gmm); 6. dark grey greenish silty clay and white concretions(CHFsm); 7. grey fine and medium sand silty matrix-supported (CH-Sm); 8. orange medium and coarse sands (CH/GB-Fsm); 9. grey coarse sands and gravel (CH/GB-Sm); 10. brown to grey silty clay, iron nodules (FF-Fsm); 11. brown sandy silt with gravels, iron nodules (FF/SB-Sm); 12. beige powdered silt (FF-Fsm); 13. sands and gravels (SB-Gcm); 14. sand, gravels and pebbles (SB-Gcm); 15. rejected age; 16. calibrated age. B. Location of boreholes; 17. “montille”; 18. borehole.

4.2. Downstream reach: Noyers-sur-Cher

4.2.1. Geometry and stratigraphy of the palaeochannel deposits

At the Noyers-sur-Cher site, the geometry of alluvial deposits was first explored through LiDAR DEM and a planimetric geophysical survey. Through the LiDAR DEM analysis, braided-like patterns were observed within the upstream meander loops and around the current riverbed (Fig. 7a). According to the location and relative elevation of this landform, a modern shift of the channel could be considered as the main explanation of this inherited morphology.

Several current channeling depressions are highlighted by LiDAR in the study area. Four were intersected by geo-archaeological trenches in the study area and named CH1, CH2, CH3a and CH3b (Fig. 7c). CH1 could be related to the last morphological type. It is a narrow channel cutting previous Holocene and Pleistocene fillings, with coarse sand and gravel deposits at the lower part that included modern ceramics and fauna (one bone was dated using ^{14}C from around 225 (± 30) yr BP, sample N1). The upper part of the filling consisted of silty deposits related to successive modern overflows. This channel could be related to the Little Ice Age climatic degradation and hydro-dynamism, which had significant impacts on fluvial morphology (Bravard, 1989; Castanet, 2008; Defive et al., 2017; Salvador et al., 2005; Salvador and Berger, 2014; Steinmann, 2015). CH2, CH3a and CH3b are shallow depressions oriented in the direction of the valley.

The planimetric electrical resistivity survey shows east–westoriented clayey fillings separated by elongated sandy/silty areas. The two main intersected clayey fillings were named CH4 and CH5 (Fig. 7d). This highlights that the geophysical tomography does not exactly match the LiDAR DEM topography, which probably reflects modern events. CH2, CH3a and CH3b cut the previous floodplain filling. CH2 was incised up to the top of the sandy base level of the floodplain filling, as seen by the more resistant area (N200 Ω·m, Fig. 7d) and the TR1 cross section (Fig. 8a). This morphology is likely related to historical overflow cutoff such as modern crevasse channels.

Channels CH4 and CH5 were investigated through trench excavation. They correspond to large and shallow depressions (about 1/ 1.20 m deep) incised in the Upper-Pleistocene sandy alluvia (SU5). CH4 is a small depression limited on the north by the cutoff of CH2 and on the south by a central sandy “montille” (Fig. 8a). Its filling has a low resistivity (20–50 Ω·m) as does CH5 (10–15 Ω·m), located in the southern-most part of the area investigated. This larger palaeochannel is limited on both sides by slight sandy “montilles” (Fig. 8b).

Similar stratigraphical successions were identified in both trenches (Figs. 8a, b, 9a and b). At the base of the channels and on the banks of the sandy “montilles”, a discontinuous coarse layer is visible, varying in thickness from 0.05 to 0.4 m and suggesting a pavement (P2, Fig. 9a and b). Indeed, the geometry of this layer (whose stratigraphy conforms with the upper limit of SU5) and composition (in which gravels are dominant) indicate a decrease in fine sand concomitant with shrinkage of the deposit, probably linked with a runoff phase. The base of channels CH4 and CH5 corresponds to a greyish-yellowish inorganic redoximorphic sandy-clay (SU4, Fig. 9c). This unit was observed within several secondary small channels nested in the larger depressions and incised in the UpperPleistocene alluvia and in the coarse sand pavement P2. A second pavement locally marks the boundary between SU3 and SU4 (P1, Fig. 9f). It is a clastic deposit composed of angular flints and quartz. Above this discontinuous unit, a deposit of organic rich black swelling clay occupied the lowest points of the palaeo-topography between the “montilles” (SU3a, Fig. 9d). This deposit may reflect the transition toward a palustrine environment and the disconnection with the main reach. The blackish aspect of this clayey unit may be acquired from subsequent pedogenesis marked by the decay of organic matter under wet conditions. Indeed, this unit holds a progressive lateral transition between a sandy facies on the “montilles” (SU3s) and a swelling clay facies at the top of the palaeochannel fillings (SU3a). Conspicuous wavy features in the cross-section that wraps the above units were initiated because of successive swelling and shrinking of the clay-dominated sediments (Fig. 9d). The stratigraphic succession ends with a sandy-silty massive deposit covering the entire plain, interpreted as alluvio-colluvium that marks the progressive regularisation of the inherited landform under surface processes (SU2).

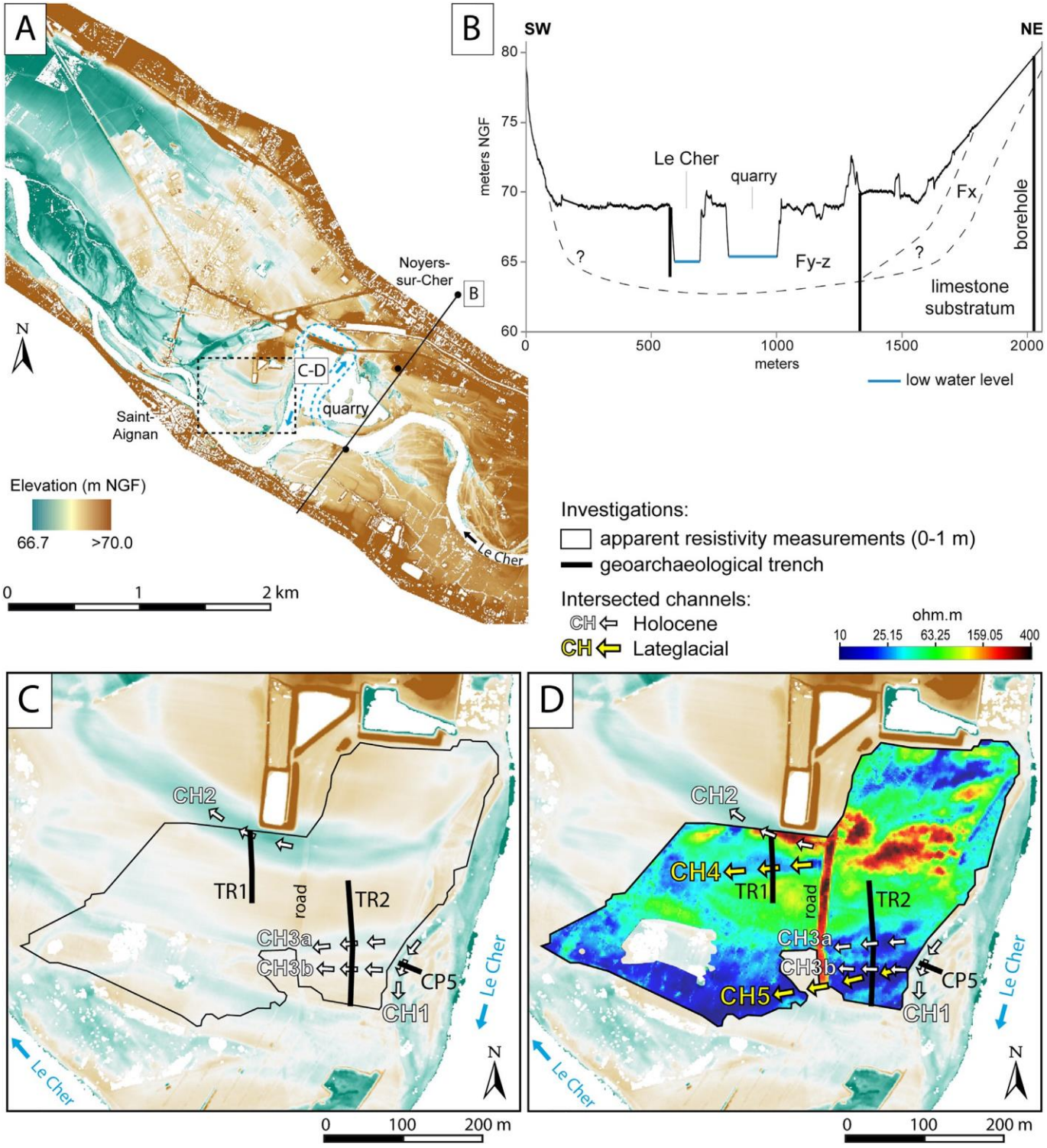

Fig. 7. Main channels within the Noyers-sur-Cher study area. A. Elevation of the valley bottom (DEM LiDAR); B. schematic cross-section of the Cher valley from DEM LiDAR and BSS-BRGM boreholes. Fx, MIS5 to MIS3 alluvia; Fy-z, MIS2 to Holocene alluvia (Alcaydé, 1994); C and D. main channels detected with DEM LiDAR (C) and resistivity map (D) in the study area. Apparent resistivity (0–1 m) (Bertholon et al., 2014).

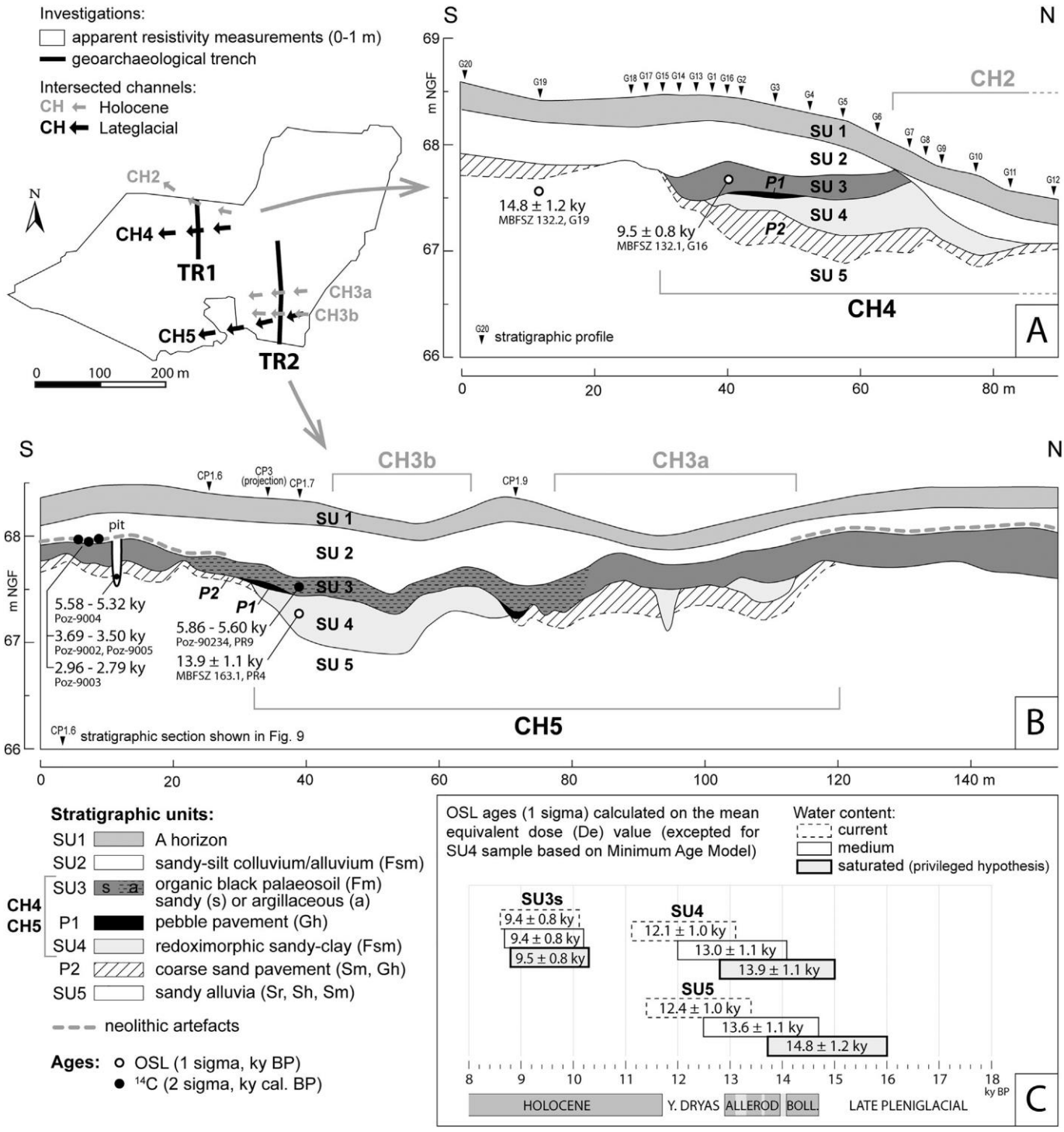

Fig. 8. Simplified cross-sections of trenches TR1 (A) and TR2 (B) within the Noyers-sur-Cher study area and distribution of the OSL (Optically Simulated Luminescence) ages (C). A and B. vertical exaggeration ×16. The four radiocarbon ages shown in the south end of TR2 are from archaeological structures located around the trench and were projected on the section respecting the stratigraphy C. chronological scale according to Rasmussen et al. (2014).

4.2.2. Palaeochannels-filling chronology

Despite a smaller portion of the floodplain studied due to the context of rescue archaeology, the fluvial geomorphological evolutions were reconstructed. According to the stratigraphic approach based on radiocarbon, OSL ages (Tables 2 and 3, Fig. 8) and archaeological data, the model of fluvial adjustments seems to follow five main steps.

(1) The top of the sandy substratum filling (SU5) was attributed to the late Pleniglacial period or the early Lateglacial according to the confidence interval (14.8 ± 1.2 ky BP, OSL age based on central age model and saturated water content). It characterises a large sedimentary load with laminar cross-bedded and small ripple marks that suggest a braided fluvial pattern (Fig. 9g). The sedimentary mobilisation may be due to slope instability and reworking processes of previous sedimentary stocks. Indeed, the site studied is located about 8 km downstream of the

confluence with the Sauldre River, one of the main tributaries whose catchment surficial lithology is dominated by sand (Tissoux et al., 2017) (Fig. 1).

(2) The SU5 phase was followed by a short period of nonsedimentation and the beginning of incision with wide area runoff (Fig. 8b). The drop in fines and shrinkage of previous deposits may have been recorded in the first coarse sand pavement (P2). The morphology of CH4 and CH5 stems from this first step. Incision continues within these wide depressions by the entrenchment of small and shallow channels in the previous pavement (P2) and the sandy substratum (SU5) (Fig. 8b). This phase may correspond to the transition between an aggradating braided fluvial pattern and an incising multiple large and shallow channel pattern.

(3) The filling of channels CH4 and CH5 occurred shortly after pavement P2. The date from SU4 likely corresponds to the Bölling/ Allerød interstadial (13.9 ± 1.1 ky BP, OSL age based on the minimum age model and saturated water content). The filling consists of inorganic sandy-clay. It probably marks the shift of the active river bed and the filling of older channels in the distal position. Slope processes suggested by inclined gravel beds (Fig. 9c) associated with inorganic nature of the sediment could denote a poorly vegetated floodplain. The transition between a multiple to single or double channels could be inferred. Occasional reactivation of the flow is recorded by pavement P1 located between SU4 and SU3. It consists of angular flint and quartz gravel, without any sandy matrix (Fig. 9f). This P1 unit may correspond to a defluviation and/or a short rise of the alluvial water table. According to the chronostratigraphy of the sequence, an attribution to the YD could be made, although it cannot be conclusively confirmed.

(4) Disconnection with the main flow is observed with SU3a. This clayey deposit located at the top of channel CH5 occurs in a distal context. It is marked by a long-run pedogenesis leading to the formation of a dark-brown vertic palaeosol. This pedogenesis affects the deposits located at the centre of the depressions as well as the top of the sandy “montilles” inherited from the Pleniglacial. This last filling is dated in CH4 from the Boreal period (9.5 ± 0.8 ky BP, OSL age based on the central age model and water-saturated content). The following pedogenesis could then be attributed to the Boreal/Atlantic period. Because of the absence of macroscopic datable remains in the SU3a, ^{14}C dating was attempted on organic matter, yielding a result between 5859 and 5601 cal. BP (sample N2), more recent than the OSL result. This ^{14}C age probably provides a minimum age to the pedogenesis. A pollen content test performed on a sample of this layer was negative. The sedimentation rate for the first part of the Holocene seems to be almost zero. The stability of the alluvial plain allowed long run pedogenesis to occur as a black palaeosol.

(5) Sedimentation restarted at least after an extensive Neolithic occupation dated ca 5500 cal. BP (sample N3) and lay on the “montilles”, at the base of SU2. Three wood charcoals found on this occupied surface and dated up to 2800 cal. BP (samples N4, N5 and N6 Fig. 8b) show that the sedimentation probably occurred later, after the Subboreal period. The SU2 is likely related to alluvio-colluvium, which may correspond to a slow and progressive regularisation of the alluvial landform, under surface processes such as bioturbation and plowing, with very little alluvial contribution. Occasional reactivation of hydrodynamism during the historical period was observed, which corresponds to the incision of CH1 (probably dated from the Little Ice Age), CH2 and CH3.

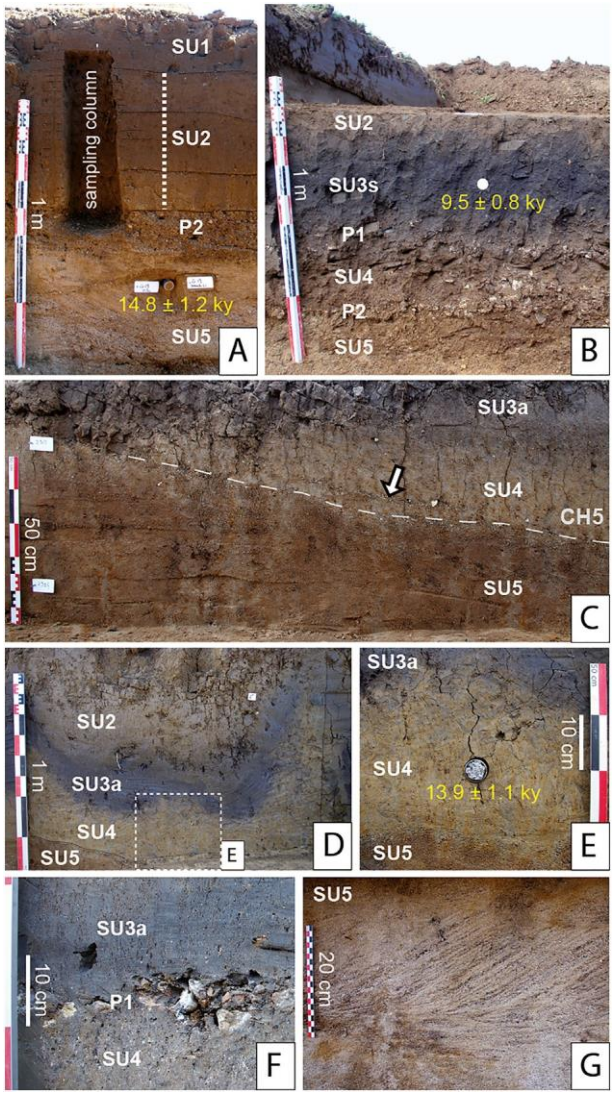

Fig. 9. Facies overview from trenches TR1 (A and B) and TR2 (C to G) within the Noyerssur-Cher study area. Legend of the stratigraphic units (SU) and location of the sections: see previous fig. A. Section G19: the OSL sample is from facies Sr; B. section G16 showing the complete channel filling sequence (CH4); C. section CP3: lateral end of channel CH5 filled by SU4 including gravel beds from SU5 (arrow); D. section CP1.7 showing postdepositional deformations by shrink-swell processes; E. detail of D; F. section CP1.9 showing pavement P1; G. section CP1.6 showing facies Sr at the top of SU5.

5. Fluvial metamorphosis, shallow incision and lateral adjustment

5.1. Signals of a smooth response to climate forcing

After presenting the morphological adjustment models of the Cher River at two points in the valley, the comparison with similar surveys conducted on fluvial systems in northwestern Europe highlights that fluvial archives from the Cher River valley depicted a smooth and progressive morphological adjustment.

5.1.1. Slight change in incision/aggradation processe

At the transition from Pleniglacial to Lateglacial, vertical reworking processes appear to be minor in the Cher valley. Neither the topographic survey through DEM LiDAR nor the stratigraphic approach conducted in both reaches studied evidenced a conspicuous entrenchment of the Pleniglacial/Lateglacial sedimentary sheet leading to the formation of a terrace. Nevertheless, an incision of channels was recorded at the transition between Pleniglacial and Lateglacial in most of the reaches investigated in the Loire valley (Castanet, 2008; Cubizolle and Georges, 2002; Morin et al., 2011; Piana et al., 2009, 2016; Steinmann, 2015; Steinmann et al., 2017; Straffin et al., 1999; Straffin and Blum, 2002) as well as in the Seine catchment (Pastre et al., 2003) and in the valleys of coastal rivers of northern France (Antoine et al., 2003; Deschodt et al., 2012) and Europe (Turner et al., 2013; Vandenberghe et al., 1987). An incision is commonly related to the milder climate of the Bölling/Allerød interstadial because of the time lag of vegetation responses after a climatic transition (Huisink, 2000; Vandenberghe, 1993).

In the same way, at the transition from the YD consisting of the last cooling episode of the Lateglacial period to the Holocene, slow and progressive reworking processes could have been suspected in the Cher River valley because of the elevation difference of bases of Lateglacial and Holocene channels, but this phenomenon is not attested. An incision was not systemically recorded in the Loire valley. However, other entrenchments of the

channels were recorded in the valleys in the northern Paris Basin (Antoine, 1997; Antoine et al., 2000, 2003, 2012; Orth et al., 2004; Pastre et al., 2000; Pastre et al., 2003).

Finally, both surveys indicated that morphological responses were mainly characterised by lateral adjustments and concentrations of flow in former reaches instead of vertical migrations.

Concerning aggradating mechanisms, an accurate specific focus conducted on palaeochannel filling at Thénioux also did not depict significant changes in sedimentation processes in response to cooler events of the Lateglacial period (MD or YD). A possible reactivation of a former channel during YD recorded in a palaeochannel in Noyers-sur-Cher was suspected, but it was not confirmed by chronologic markers. During this YD, fluvial systems located in the northern part of the Paris basin (Seine and Somme) experienced a major phase of slope erosion, inducing chalky deposition in the floodplains (Antoine, 1997; Antoine et al., 2000, 2003, 2012; Pastre et al., 2000; Pastre et al., 2003). Other reaches studied recorded an increase in grain size interpreted as a response to contrasted discharges associated with periglacial conditions (Bertran et al., 2009; Castanet, 2008).

5.1.2. Change in fluvial pattern

The current river is characterised by low-energy meanders (Dépret et al., 2017, 2015). Sinuous and meandering channels were the dominant fluvial pattern during the second half of the Holocene (Vayssière, 2018; Vayssière et al., 2016). The occurrence of a fluvial metamorphosis was recorded through deposits of the Lateglacial period. The braided system evolves toward a transitional pattern characterised by one or two wide, shallow, straight channels located in former braided reaches. These deposits were reworked by Holocene meanders because of lateral erosion. According to the survey conducted in Noyers-sur-Cher, the evolution from a braided toward a transitional pattern was recorded around 14.8 ± 1.2 ky BP at the latest. At Thénioux, such transitional channels are abandoned at approximatively the same time (15179–14,674 cal. BP and 13,940–13,553 cal. BP). Markers of a completed fluvial metamorphosis characterised by a single-thread sinuous or meandering channel were recorded ca 6 ky cal. BP at Thénioux and during the LIA at Noyers-sur-Cher (Fig. 10).

No other phenomenon of fluvial metamorphosis was observed. This planform adjustment, implying a transition through a braided to a meandering system, is consistent with the elaborated model through previous investigations conducted in western European valleys (Antoine et al., 2003; Pastre et al., 2003; Straffin et al., 1999; Straffin and Blum, 2002; Vandenberghe et al., 1987). Nevertheless, several changes in fluvial morphology can be identified during the Lateglacial period, as was shown in the Burgundian Loire (upstream part of the lowland Loire valley) that is closer to the mountainous area and to sedimentary sources (Steinmann, 2015; Steinmann et al., 2017) or in other catchments of western Europe, especially during the cooler YD episode (Vandenberghe et al., 1994).

5.2. Exploring factors explaining the lack of strong morphogenetic processes

The previous comparison with known geomorphological evolution patterns of adjacent fluvial systems reinforces the idea that morphological adjustments of the Cher River are part of an original model. To what extent can the specificities of the reaches studied explain this adjustment of fluvial landforms during the Lateglacial period?

5.2.1. Intrinsic components of the basin

First, intrinsic components of the basin (slope and width) could explain the lack of conspicuous morphogenetic processes (weak aggradation of the floodplain, slight incision and reworking mechanisms) at the end of the Lateglacial period and during the early Holocene. Slope and valley floor width are physiographic properties that we can consider as determining factors for morphogenetic mechanisms (Schumm, 1977). Indeed, flow energy and associated reworking processes are mostly determined by steepness (Houben, 2003; Mol et al., 2000; Vandenberghe, 1995; Vandenberghe et al., 1994). In addition, Houben (2003) emphasised that large valley width and low-gradient sections correspond to a physiographic configuration that would increase sedimentation rates and minimise reworking probabilities.

Considering the gradient of the valley, Noyers-sur-Cher and Thénioux are located in a homogenous reach where the valley slope seems to be poorly contrasted (Fig. 2). This configuration could have inhibited reworking processes and the entrenchment of subsequent channels in Pleistocene deposits. For comparison, no sedimentary formations have been attributed to the Lateglacial or to the early Holocene at the Bigny site where the floodplain is almost completely occupied by a late Holocene meander belt (Vayssière, 2018; Vayssière et al., 2016). This site is located in the upper part of the middle valley where the slope is slightly higher (0.83 $m \cdot km^{-1}$) and where there is an alternation of steep and less steep sections (Fig. 2). Furthermore, the sharp widening of the valley floor at Thénioux could have promoted the preservation of thicker Lateglacial deposits trapped in palaeochannels in comparison with the Noyers-sur-Cher site (Fig. 2).

The Noyers-sur-Cher and Thénioux sites closely fit the model proposed by Mol et al. (2000) and Houben (2003). Nevertheless, more detailed surveys conducted in the Cher River valley regarding basin properties are needed to fully understand how intrinsic components affect fluvial adjustments during Lateglacial.

5.2.2. Spatial and topographical gradients

The geographical location of the reaches studied could also have led to more moderated climatic oscillations. The comparison with surveys conducted in northwestern Europe allow the location of sites to be analysed. We can suppose that low elevation and a location farther south and west could have resulted in less pronounced periglacial conditions (stability of permafrost area and duration of seasonal frozen soil, slight opening-up of forests) during cooler episodes of the Lateglacial. Smoother periglacial conditions in the Cher valley could have reduced cryoclastic processes. The lack of ice-wedges in the Cher basin witnesses the limited effect of the periglacial climate. In France, deformations related to ice wedges would

be less widespread below 47°N (Andrieux et al., 2016). The Thénioux and Noyers-sur-Cher sites are located on the edge of this area (47.252 and 47.16°N, respectively). These attenuated mechanisms could have preserved the fluvial environment from morphogenetic instability. Concerning the elevation gradient, an investigation conducted in the mountainous part of the Loire River catchment found a sedimentary record mainly focused on the last two millennia (Defive et al., 2017). Nevertheless, investigations conducted in the upstream lowland area of the Loire catchment clearly described developed Lateglacial sedimentary succession (Steinmann, 2015; Steinmann et al., 2017; Straffin et al., 1999; Straffin and Blum, 2002) and an earlier incision at the beginning of the Lateglacial (Cubizolle and Georges, 2002; Steinmann, 2015; Steinmann et al., 2017).

The comparison with studies conducted in reaches farther north such as the Middle Loire valley, the Seine and the Somme catchments (Antoine, 1997; Antoine et al., 2012, 2003, 2000; Castanet, 2008; Pastre et al., 2003; Pastre et al., 2000) show a more pronounced response (successive floodplain aggradation and incision, hillslope runoff and erosion) to Lateglacial climatic oscillations. This gradient could also have enhanced the fluvial response of river farther north because of the abundant loess cover, which can support a fine sediment supply and promote the aggradation of the valley bottom. The sediment supply is likely to be different in the Cher River catchment since the loess cover is less developed. However, few surveys are available concerning the lowland fluvial system located farther south, making it difficult to confirm this hypothesis. Investigations conducted in a tributary of the Dordogne River in the Aquitanian basin suggest an increase in coarse sediment deposition during the MD (the YD does not seem to be recorded) (Bertran et al., 2009).

Hence, the comparison with previous surveys regarding their eastwest location could have led to the hypothesis of less pronounced periglacial conditions because of a climatic gradient. Indeed, fluvial adjustments of the Cher River could be related with those of the downstream Loire and of the Choisille River. Slow and progressive adaptations of fluvial landforms were recorded in both reaches during the Lateglacial (Carcaud, 2004; Carcaud et al., 2002; Morin et al., 2011). These sites are located farther west and could have been affected by – apart from local topographic conditions - balanced climatic oscillations because of the more oceanic climate.

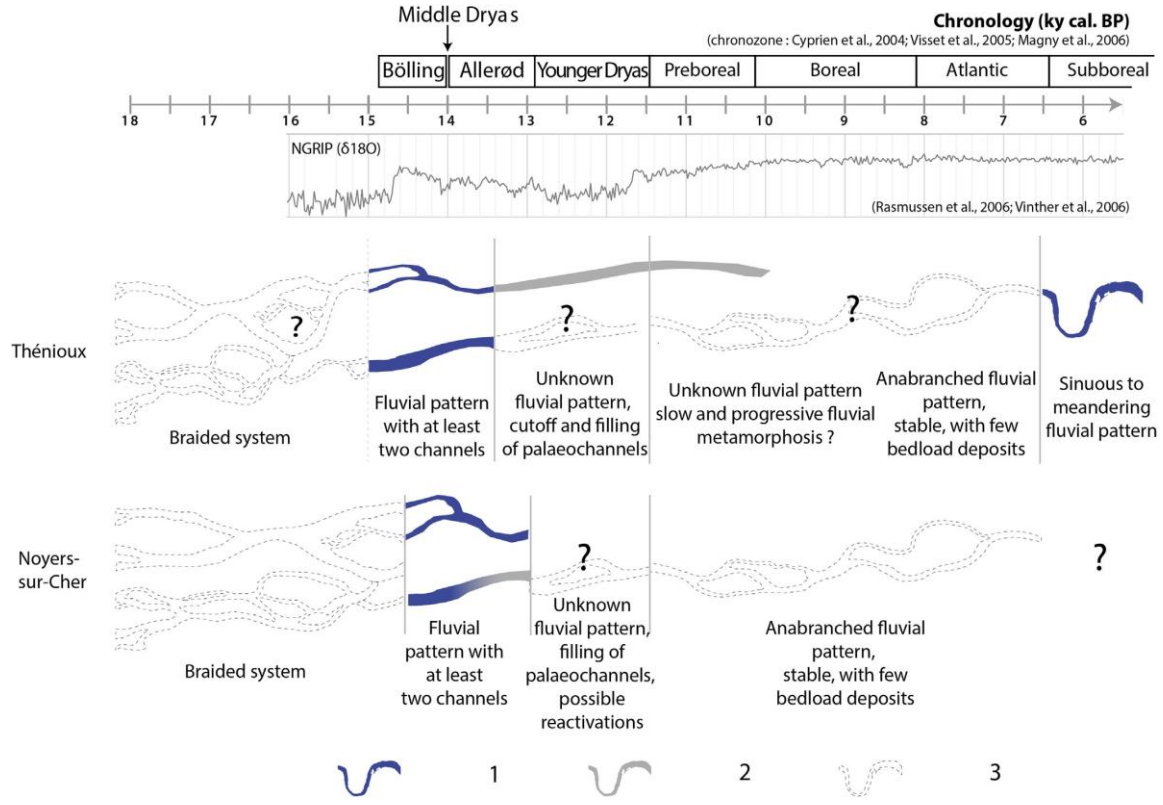

Fig. 10. Synthesis of fluvial morphology adjustment at Thénioux and Noyers-sur-Cher during Lateglacial and early Holocene. 1. attested active channel; 2. confirmed abandoned channel; 3. suspected fluvial pattern. (Cyprien et al., 2004; Magny et al., 2006; Rasmussen et al., 2006; Vinther et al., 2006; Visset et al., 2005).

6. Conclusions

This study is a contribution to the knowledge of fluvial responses to climatic oscillations of the Lateglacial through the investigation of two reaches located in the lowland area of a medium-sized catchment. At Thénioux, during the early Lateglacial, fluvial morphology corresponds to a transitional pattern composed of at least two straight channels including one main arm and lateral channel(s). During the Bölling and Allerød interstadials, side channels were abandoned and filled with organic silt and peaty deposition. Fluvial archives attributed to YD and early Holocene consist of lithogenic silty deposits formed in a distal context trapped into former side arms affected by dewatering and pedogenetic processes. No significant changes in sedimentation processes in response to climatic oscillations were identified. The transition toward a meandering pattern was recorded around 5888–5652 cal. BP at the latest. At Noyers-sur-Cher, after 14.8 ± 1.2 ky BP, wide and shallow channels were formed, slightly incising previous sandy formations. They are filled with inorganic sandy-clay materials during the Bölling/Allerød interstadial. The first part of the Holocene is marked by a

black clayey layer dated of the Boreal period and affected by long-run pedogenesis. The total thickness of this infilling sequence is small, always inframetric.

Through the assessment of geomorphological trajectories of the two reaches studied, we highlight that fluvial metamorphosis occurring during the Lateglacial and the early Holocene seems to be characterised by lateral readjustments and a low signal of morphological instability (shallow incision, weak aggradation processes, slow and progressive change in channel morphology). This observation is enhanced by the comparison with known geomorphological evolution patterns of adjacent basins. First, the slope and the valley width were considered as major explanation for the lack of morphogenetic processes. Then, the low elevation as well as the location farther south and west may also have led to less pronounced periglacial conditions explaining reduced geomorphological adjustments. In addition, the less developed loess cover may have limited the fine sediment supply and the subsequent aggradation of the valley bottom.

Acknowledgments

At Noyers-sur-Cher, field investigations could not have taken place without the participation of the company Les Matériaux du Cher, the Service Régional de l'Archéologie (Centre-Val de Loire region), the company Geocarta, the Institut National de Recherches Archéologiques Préventives and the company Paléotime. We thank the supervisors of the archaeological excavations, which been undertaken on the meander of Le Busa since 2008: Nasser Djemmali, Fiona Kildea (Inrap), Régis Picavet, Harold Lethrosne (Paléotime), and all the field teams. The research carried out at Thénioux and Bigny is associated with the investigation themes of the Zone Atelier Loire (CNRS-INEE). It is also part of the AGES-Ancient Geomorphological EvolutionS research programme (coordination: Cyril Castanet, 2013–2016) funded by the European Union (FEDER), the Agence de l'Eau Loire-Bretagne and the Etablissement Public Loire. The quality and focus of this manuscript were greatly improved by suggestions from Jef Vandenberghe and one anonymous reviewer.

References

Adamiec, G., Aitken, M.J., 1998. Dose-rate conversion factors: update. Anc. TL 37–50.

Aitken, M.J., 1985. Thermoluminescence Dating. Academic Press. ed, Londres.

Aitken, M.J., 1998. Introduction to Optical Dating: The Dating of Quaternary Sediments by the Use of Photon-Stimulated Luminescence. Oxford University Press, Oxford, New York.

Alcaydé, G., 1994. Carte géologique de la France, Feuille 516 (Châtillon-sur-Indre).

Andrieux, E., Bertran, P., Saito, K., 2016. Spatial analysis of the French Pleistocene permafrost by a GIS database. Permafr. Periglac. Process. 27, 17–30. https://doi.org/10.1002/ ppp.1856.

Antoine, P., 1997. Modifications des systèmes fluviatiles à la transition PléniglaciaireTardiglaciaire et à l'Holocène: l'exemple du bassin de la Somme (Nord de la France). Géographie Phys. Quat. 51, 93. https://doi.org/10.7202/004763ar.

Antoine, P., Fagnart, J.P., Limondin-Lozouet, N., Munaut, A.V., 2000. Le Tardiglaciaire du bassin de la Somme: éléments de synthèse et nouvelles données [the Lateglacial from the Somme basin: first synthesis and new data]. Quaternaire 11, 85–98. https://doi.org/10.3406/quate.2000.1658.

Antoine, P., Munaut, A.-V., Limondin-Lozouet, N., Ponel, P., Dupéron, J., Dupéron, M., 2003. Response of the Selle River to climatic modifications during the Lateglacial and Early Holocene (Somme Basin-Northern France). Quat. Sci. Rev. Fluvial response to rapid environmental change 22, 2061–2076. https://doi.org/10.1016/S0277-3791(03) 00180-X.

Antoine, P., Fagnart, J.P., Auguste, P., Coudret, P., Limondin-Lozouet, N., Ponel, P., Munaut, A.V., Defgnée, A., Gauthier, A., Fritz, C., 2012. Conty, vallée de la Selle (Somme, France): séquence tardiglaciaire de référence et occupations préhistoriques. Quaternaire, hors-série n°5, Quaternaire.

Bertholon, J., Galland, D., Dabas, M., 2014. Rapport de cartographie géophysique, Noyerssur-Cher (41), lieu-dit Le Busa. Géocarta, Paris.

Bertran, P., Allenet, G., Fourloubey, C., Leroyer, C., Limondin-Lozouet, N., Maazouzi, Z., Madelaine, S., Perrière, J., Ponel, P., Casagrande, F., Detrain, L., 2009. Paléoenvironnements tardiglaciaires en Aquitaine: la séquence alluviale de la Brunetière (Bergerac, France). Quaternaire. 161–193. https://doi.org/10.4000/ quaternaire.5107.

Bertran, P., Liard, M., Sitzia, L., Tissoux, H., 2016. A map of Pleistocene aeolian deposits in Western Europe, with special emphasis on France. J. Quat. Sci. 31, 844–856. https://doi.org/10.1002/jqs.2909.

Blott, S.J., Pye, K., 2001. GRADISTAT: a grain size distribution and statistics package for the analysis of unconsolidated sediments. Earth Surf. Process. Landf. 26, 1237–1248. https://doi.org/10.1002/esp.261.

Bohncke, S.J.P., Vandenberghe, J., Huijzer, A.S., 1993. Periglacial environments during the Weichselian Late Glacial in the Maas valley, the Netherlands. Neth. J. Geosci. - Geol. En Mijnb. 72, 193–210.

Bohncke, S.J.P., Kasse, C., Vandenberghe, J., 1995. Climate induced environmental changes during the Vistulian Lateglacial at Zabinko, Poland. Quaest. Geogr. 4, 43–64.

Bravard, J.P., 1989. La métamorphose des rivières des Alpes françaises à la fin du MoyenAge et à l'époque moderne. Bull. Soc. Geogr. Liege 145–157.

Bronk Ramsey, C., 2009. Bayesian analysis of radiocarbon dates. Radiocarbon 51, 337–360. https://doi.org/10.1017/S0033822200033865.

Brown, A.G., Lespez, L., Sear, D.A., Macaire, J., Houben, P., Klimek, K., Brazier, R.E., Van Oost, K., Pears, B., 2018. Natural vs anthropogenic streams in Europe: history, ecology and implications for restoration, river-rewilding and riverine ecosystem services. EarthSci. Rev. 180, 185–205. https://doi.org/10.1016/j.earscirev.2018.02.001.

Carcaud, N., 2004. D'espace et de temps: un itinéraire de recherche et d'enseignement sur les anthroposystème fluviaux, mémoire d'HDR. ed. Université d'Angers.

Carcaud, N., Garcin, M., Visset, L., Musch, J., Burnouf, J., 2002. Nouvelles lectures de l'évolution des paysages fluviaux à l'Holocène dans le bassin de la Loire moyenne, in: Les Fleuves Ont Une Histoire, Paléo-Environnement Des Rivières et Des Lacs Français Depuis 15 000 Ans (Dir. Bravard J-P., Magny M.). Errance, 71–84.

Castanet, C., 2008. La Loire en val d'Orléans: dynamiques fluviales et socioenvironnementales durant les derniers 30 000 ans (PhD thesis). Université Panthéon-Sorbonne, Paris, France.

Cubizolle, H., Georges, V., 2002. Evolution morphosédimentaire des plaines alluviales de la Loire et de ses affluents dans le bassin du Forez (Massif Central français) depuis la fin du Würm, in: Les Fleuves Ont Une Histoire. Paléo-Environnements Des Rivières et Des Lacs Français Depuis 15 000 Ans, (Dir. Bravard J-P., Magny M.). Errance, 63–70.

Cyprien, A.-L., Visset, L., Carcaud, N., 2004. Evolution of vegetation landscapes during the Holocene in the central and downstream Loire basin (Western France). Veg. Hist. Archaeobotany 13, 181–196. https://doi.org/10.1007/s00334-004-0042-y.

Dabas, M., 2009. Theory and practice of the new fast electrical imaging system ARP, in: Seeing the Unseen. Geophysics and Landscape Archaeology (Dir. Campana S. and Piro S.). pp. 105–126.

Define, E., Berger, J.-F., Poiraud, A., Barra, A., Bouvard, E., Virmoux, C., Voldoire, O., Garreau, A., Miras, Y., Beauger, A., Cabanis, M., Gunnell, Y., Braucher, R., Dendievel, A.-M., Nomade, S., Delvigne, V., Lafarge, A., Liabeuf, R., Guillou, H., Raynal, J.-P., 2017. Les flux hydro-sédimentaires dans le bassin supérieur du fleuve Loire (Massif Central, France) au cours des trois derniers millénaires: archives séquentielles, chronologie et corrélations régionales. Quaternaire, 373–388 https://doi.org/10.4000/ quaternaire.8304.

Dépret, T., Gautier, E., Hooke, J., Grancher, D., Virmoux, C., Brunstein, D., 2015. Hydrological controls on the morphogenesis of low-energy meanders (Cher River, France). J. Hydrol. 531, 877–891. https://doi.org/10.1016/j.jhydrol.2015.10.035.

Dépret, T., Gautier, E., Hooke, J., Grancher, D., Virmoux, C., Brunstein, D., 2017. Causes of planform stability of a low-energy meandering gravel-bed river (Cher River, France). Geomorphology 285, 58–81. https://doi.org/10.1016/j.geomorph.2017.01.035.

Deschodt, L., Salvador, P.-G., Feray, P., Schwenninger, J.-L., 2012. Transect partiel de la plaine de la Scarpe (bassin de l'Escaut, nord de la France). Stratigraphie et évolution paléogéographique du Pléniglaciaire supérieur à l'Holocène récent. Quaternaire, 87–116 https://doi.org/10.4000/quaternaire.6116.

Despriée, J., Voinchet, P., Bahain, J.-J., Tissoux, H., Falguères, C., Dépont, J., Dolo, J.-M., 2007. Les nappes alluviales pléistocènes de la vallée moyenne du Cher (Région Centre, France): contexte morphosédimentaire, chronologie ESR et Préhistoire. Premiers résultats. Quaternaire 349–368. doi:https://doi.org/10.4000/quaternaire.1225.

Galbraith, R.F., Green, P.F., 1990. Estimating the component ages in a finite mixture. Int.J. Radiat. Appl. Instrum. Part Nucl. Tracks Radiat. Meas. 17, 197–206. https://doi.org/10.1016/1359-0189(90)90035-V.

Galbraith, R.F., Roberts, R.G., Laslett, G.M., Yoshida, H., Olley, J.M., 1999. Optical dating of single and multiple grains of quartz from Jinmium rock shelter, northern Australia: part I, experimental design and statistical models. Archaeometry 41, 339–364.
Genelle, F., Sirieix, C., Riss, J., Naudet, V., Dabas, M., Bégassat, P., 2014. Detection of landfill cover damage using geophysical methods. Surf. Geophys. 12, 599–611. https://doi. org/10.3997/1873-0604.2014018.
Harwood, K., Brown, A.G., 1993. Fluvial processes in a forested anastomosing river: Flood partitioning and changing flow patterns. Earth Surf. Process. Landf. 18, 741–748. https://doi.org/10.1002/esp.3290180808.
Houben, P., 2003. Spatio-temporally variable response of fluvial systems to Late Pleistocene climate change: a case study from Central Germany. Quat. Sci. Rev. Fluvial response to rapid environmental change 22, 2125–2140. https://doi.org/10.1016/ S0277-3791(03)00181-1.
Huisink, M., 1997. Late-glacial sedimentological and morphological changes in a lowland river in response to climatic change: the Maas, southern Netherlands. J. Quat. Sci. 12, 209–223. https://doi.org/10.1002/(SICI)1099-1417(199705/06)12:3b209::AIDJQS306N3.0.CO;2-P.
Huisink, M., 2000. Changing river styles in response to Weichselian climate changes in the Vecht valley, eastern Netherlands. Sediment. Geol. 133, 115–134. https://doi.org/ 10.1016/S0037-0738(00)00030-0.
Kasse, C., 1998. Depositional model for cold-climate tundra rivers, in: Palaeohydrology and Environmental Change (Dir. Benito G., Baker V.R. and Gregory K.J.). Chichester, pp. 83–97.
Kasse, C., Vandenberghe, J., Bohncke, S.J.P., 1995. Climatic change and fluvial dynamics of the Maas during the late Weichselian and Early Holocene. Eur. River Act. Clim. Change Lateglacial Early Holocene PaläoklimaforschungPalaeoclimate Res. Vol 14 Spec. Issue ESF Proj. Eur. Palaeoclim. Man 9, 123–150.
Kasse, C., Vandenberghe, D., De Corte, F., Van Den Haute, P., 2007. Late Weichselian fluvioaeolian sands and coversands of the type locality Grubbenvorst (southern Netherlands): sedimentary environments, climate record and age. J. Quat. Sci. 22, 695–708. https://doi.org/10.1002/jqs.1087.
Konert, M., Vandenberghe, J., 1997. Comparison of laser grain size analysis with pipette and sieve analysis: a solution for the underestimation of the clay fraction. Sedimentology 44, 523–535. https://doi.org/10.1046/j.1365-3091.1997.d01-38.x.
Larue, J.-P., 1981. Les nappes alluviales de la vallée du Cher dans le bassin de Montluçon. Norois 111, 345–360. https://doi.org/10.3406/noroi.1981.3972.
Leroyer, C., Allenet de Ribemont, G., Chaussé, C., 2014. Le paysage végétal durant le Tardiglaciaire: Bazoche-lès-Bray, une référence pour le site de Pincevent. Un Automne à Pincevent, Le Campement Magdalénien Du Niveau IV20 (Dir. Julien M., Karlin C.).
Lespez, L., Viel, V., Rollet, A.-J., Delayaye, D., 2015. The anthropogenic nature of presentday low energy rivers in western France and implications for current restoration projects. Geomorphology 251, 64–76. https://doi.org/10.1016/j.geomorph.2015.05.015.
Loke, M.-H., 1999. Electrical Imaging Surveys Forenvironmental and Engineering Studies, a Practical Guide to 2-D and 3-D Surveys.
Magny, M., Aalbersberg, G., Bégeot, C., Benoit-Ruffaldi, P., Bossuet, G., Disnar, J.-R., Heiri, O., Laggoun-Defarge, F., Mazier, F., Millet, L., Peyron, O., Vannière, B., WalterSimonnet, A.-V., 2006. Environmental and climatic changes in the Jura mountains (eastern France) during the Lateglacial–Holocene transition: a multi-proxy record from Lake Lautrey. Quat. Sci. Rev. 25, 414–445. https://doi.org/10.1016/j. quascirev.2005.02.005.
Manivit, J., Debrand-Passard, S., Gros, Y., Desprez, N., 1994. Carte géologique et notice explicative de la feuille Vierzon au 1/50 000.
Marescot, L., 2006. Introduction à l'imagerie électrique du sous-sol. Bull. Soc. Vaud. Sci. Nat. 90, 23–40.
Miall, A.D., 1996. The Geology of Fluvial Deposits: Sedimentary Facies, Basin Analysis, and Petroleum Geology, 1st ed. 1996. Corr. 3rd printing 2006. ed. Springer-Verlag Berlin and Heidelberg GmbH & Co. K, Berlin; New York.
Mol, J., Vandenberghe, J., Kasse, C., 2000. River response to variations of periglacial climate in mid-latitude Europe. Geomorphology 33, 131–148. https://doi.org/10.1016/ S0169-555X(99)00126-9.
Morin, E., Macaire, J.-J., Hinschberger, F., Gay-Ovéjéro, I., Rodrigues, S., Bakyono, J.-P., Visset, L., 2011. Spatio-temporal evolution of the Choisille River (southern Parisian Basin, France) during the Weichselian and the Holocene as a record of climate trend and human activity in North-Western Europe. Quat. Sci. Rev. 30, 347–363. https://doi.org/10.1016/j.quascirev.2010.11.015.
Nanson, G.C., Knighton, A.D., 1996. Anabranching rivers: their cause, character and classification. Earth Surf. Process. Landf. 21, 217–239. https://doi.org/10.1002/(SICI)10969837(199603)21:3b217::AID-ESP611N3.0.CO;2-U.
Notebaert, B., Verstraeten, G., Govers, G., Poesen, J., 2009. Qualitative and quantitative applications of LiDAR imagery in fluvial geomorphology. Earth Surf. Process. Landf. 34, 217–231. https://doi.org/10.1002/esp.1705.
Orth, P., Pastre, J., Gauthier, A., Limondin-Lozouet, N., Kunesch, S., 2004. Les enregistrements morphosédimentaires et biostratigraphiques des fonds de vallée du bassin-versant de la Beuvronne (Bassin parisien, Seine-et-Marne, France): perception des changements climatoanthropiques à l'Holocène[Holocene morphosedimentary and bio-stratigraphy records from alluvial fills of the Beuvronne river catchment (Paris basin, France): perception of climatic changes and human activities.]. Quaternaire 15, 285–298. https://doi.org/10.3406/quate.2004.1775.
Pastre, J.-F., Leroyer, C., Limondin-Lozouet, N., Chaussé, C., Fontugne, M., Gebhardt, A., Hatté, C., Krier, V., 2000. Le Tardiglaciaire des fonds de vallée du Bassin Parisien (France). Quaternaire 11, 107–122. https://doi.org/10.3406/quate.2000.1660.
Pastre, J.-F., Limondin-Lozouet, N., Leroyer, C., Ponel, P., Fontugne, M., 2003. River system evolution and environmental changes during the Lateglacial in the Paris Basin (France). Quat. Sci. Rev. Fluvial response to rapid environmental change 22, 2177–2188. https://doi.org/10.1016/S0277-3791(03)00147-1.
Piana, J., Carcaud, N., Cyprien-Chouin, A.-L., Visset, L., Leroy, D., 2009. Dynamique paysagère tardiglaciaire et holocène dans la vallée du Loir à Pezou (Loir-et-Cher): développements méthodologiques et premiers résultats. Norois Environ. Aménage. Société, 73–88 https://doi.org/10.4000/norois.3047.
Piana, J., Carcaud, N., Castanet, C., 2016. Géoarchéologie de la vallée du Loir: dynamiques fluviales Tardiglaciaire et Holocène, interactions sociétés/milieux, in: Rapport Scientifique Du Programme AGES (Ancient Geomorphological EvolutionS)- Evolutions Géomorphologiques Anciennes de l'hydrosystème Ligérien, 333–357.
Prescott, J.R., Hutton, J.T., 1994. Cosmic ray contributions to dose rates for luminescence and ESR dating: large depths and long-term time variations. Radiat. Meas. 23, 497–500. https://doi.org/10.1016/1350-4487(94)90086-8.
Prescott, J.R., Stephan, L.G., 1982. The contribution of cosmic radiation to the environmental dose for thermoluminescent dating. Latitude, altitude and depth dependences. PACT 17–25.
Rasmussen, S.O., Andersen, K.K., Svensson, A.M., Steffensen, J.P., Vinther, B.M., Clausen, H.B., Siggaard-Andersen, M.-L., Johnsen, S.J., Larsen, L.B., Dahl-Jensen, D., Bigler, M., Röthlisberger, R., Fischer, H., Goto-Azuma, K., Hansson, M.E., Ruth, U., 2006. A new Greenland ice core chronology for the last glacial termination. J. Geophys. Res.Atmos. 111. https://doi.org/10.1029/2005JD006079.
Rasmussen, S.O., Bigler, M., Blockley, S.P., Blunier, T., Buchardt, S.L., Clausen, H.B., Cvijanovic, I., Dahl-Jensen, D., Johnsen, S.J., Fischer, H., Gkinis, V., Guillevic, M., Hoek, W.Z., Lowe, J.J., Pedro, J.B., Popp, T., Seierstad, I.K., Steffensen, J.P., Svensson, A.M., Vallelonga, P., Vinther, B.M., Walker, M.J.C., Wheatley, J.J., Winstrup, M., 2014. A stratigraphic framework for abrupt climatic changes during the last Glacial period based on three synchronized Greenland ice-core records: refining and extending the INTIMATE event stratigraphy. Quat. Sci. Rev., Dating, Synthesis, and Interpretation of Palaeoclimatic Records and Model-data Integration: advances of the INTIMATE project(INTegration of Ice core, Marine and TErrestrial records, COST Action ES0907) 106, 14–28. doi:https://doi.org/ 10.1016/j.quascirev.2014.09.007.
Reimer, P.J., Bard, E., Bayliss, A., Beck, J.W., Blackwell, P.G., Ramsey, C.B., Buck, C.E., Cheng, H., Edwards, R.L., Friedrich, M., Grootes, P.M., Guilderson, T.P., Haflidason, H., Hajdas, I., Hatté, C., Heaton, T.J., Hoffmann, D.L., Hogg, A.G., Hughen, K.A., Kaiser, K.F., Kromer, B., Manning, S.W., Niu, M., Reimer, R.W., Richards, D.A., Scott, E.M., Southon, J.R., Staff, R.A, Turney, C.S.M., van der Plicht, J., 2013. IntCal13 and Marine13 Radiocarbon Age Calibration Curves 0–50,000 years cal BP. Radiocarbon 55, 1869–1887. https://doi. org/10.2458/azu_js_rc.55.16947.
Renssen, H., Seppä, H., Heiri, O., Roche, D.M., Goosse, H., Fichefet, T., 2009. The spatial and temporal complexity of the Holocene thermal maximum. Nat. Geosci. 2, 411–414. https://doi.org/10.1038/ngeo513.
Richards, K., 2004. Rivers: Form and Process of Alluvial Channels. The Blackburn Press, Caldwell, N.J.
Salvador, P.-G., Berger, J.-F., 2014. The evolution of the Rhone River in the Basses Terres basin during the Holocene (Alpine foothills, France). Geomorphology 204, 71–85. https://doi.org/10.1016/j.geomorph.2013.07.030.
Salvador, P.-G., Berger, J.-F., Fontugne, M., Gauthier, É., 2005. Etude des enregistrements sédimentaires holocènes des paléoméandres du Rhône dans le secteur des basses terres (Ain, Isère, France). Quaternaire, 315–327 https://doi. org/10.4000/quaternaire.517.
Schumm, S.A., 1977. The Fluvial System. Blackburn Press.
Schumm, S.A., 1979. Geomorphic thresholds: the concept and its applications. Trans. Inst.
Br. Geogr. 4, 485–515. https://doi.org/10.2307/622211.
Steinmann, R., 2015. L'influence climatique et anthropique sur trois cours d'eaux bourguignons: géoarchéologie de sites de franchissement sur la Loire, la Saône et le Doubs au cours de l'Holocène (PhD thesis). Université de Bourgogne.
Steinmann, R., Garcia, J.-P., Dumont, A., Quiquerez, A., 2017. Aspects méthodologiques de l'approche intégrée des comblements postglaciaires: apports pour la reconstitution de la dynamique fluviale de la Loire au cours de l'Holocène. Géomorphologie Relief Process. Environ. 23, 83–104. https://doi.org/10.4000/geomorphologie.11650.
Straffin, E., Blum, M., 2002. Late and post-glacial fluvial dynamics of the Loire river, Burgundy, France, in Les fleuves ont une histoire, in: Paléo-Environnement Des Rivières et Des Lacs Français Depuis 15 000 Ans, (Dir. Bravard J-P; Magny M.). Errance, 85–99.
Straffin, E., Blum, M., Colls, A., Stokes, S., 1999. Alluvial stratigraphy of the Loire and

Arroux rivers (Burgundy, France) [Stratigraphie des alluvions de la Loire et de l 'Arroux, Bourgogne, France]. Quaternaire 10, 271–282. https://doi.org/10.3406/ quate.1999.1648.
Tissoux, H., Prognon, F., Martelet, G., Tourliere, B., Despriée, J., Liard, M., Lacquement, F., 2017. Interprétation d'un levé de spectrométrie gamma pour la connaissance des dépôts silico-clastiques fluviatiles en centre France (Loire et Sologne). Quaternaire, 87–103 https://doi.org/10.4000/quaternaire.7848.
Turner, F., Tolksdorf, J.F., Viehberg, F., Schwalb, A., Kaiser, K., Bittmann, F., von Bramann, U., Pott, R., Staesche, U., Breest, K., Veil, S., 2013. Lateglacial/early Holocene fluvial reactions of the Jeetzel river (Elbe valley, northern Germany) to abrupt climatic and environmental changes. Quat. Sci. Rev. 60, 91–109. https://doi.org/10.1016/j. quascirev.2012.10.037.
Udden, J.-A., 1914. Mechanical composition of clastic sediments. Bull. Geol. Soc. Am. 25, 655–744.
Vandenberghe, J., 1993. Changing fluvial processes under changing periglacial conditions. Z. Für Geomorphol. 17–28.
Vandenberghe, J., 1995. The role of rivers in palaeoclimatic reconstruction. Eur. River Act. Clim. Change Lateglacial Early Holocene PaläoklimaforschungPalaeoclimate Res. Vol 14 Spec. Issue ESF Proj. Eur. Palaeoclim. Man 9, 11–19.
Vandenberghe, J., 2003. Climate forcing of fluvial system development: an evolution of ideas. Quat. Sci. Rev. 22, 2053–2060. https://doi.org/10.1016/S0277-3791(03) 00213-0.
Vandenberghe, J., 2008. The fluvial cycle at cold–warm–cold transitions in lowland regions: a refinement of theory. Geomorphology 98, 275–284. https://doi.org/ 10.1016/j.geomorph.2006.12.030.
Vandenberghe, J., Woo, M., 2002. Modern and ancient periglacial river types. Prog. Phys.
Geogr. Earth Environ. 26, 479–506. https://doi.org/10.1191/0309133302pp349ra.
Vandenberghe, J., Bohncke, S., Lammers, W., Zilverberg, L., 1987. Geomorphology and palaeoecology of the Mark valley (southern Netherlands): geomorphological valley development during the Weichselian and Holocene. Boreas 16, 55–67. https://doi.org/ 10.1111/j.1502-3885.1987.tb00754.x.
Vandenberghe, J., Kasse, C., Bohncke, S., Kozarski, S., 1994. Climate-related river activity at the Weichselian-Holocene transition: a comparative study of the Warta and Maas rivers. Terra Nova 6, 476–485. https://doi.org/10.1111/j.13653121.1994.tb00891.x.
Vayssière, A., 2018. Trajectoire et processus fluviaux dans la moyenne vallée du Cher du Tardiglaciaire à la période actuelle: Métamorphose fluviale, réponses aux forçages sociétaux et ajustements des chenaux et des bras morts (PhD thesis). Université Paris 1 Panthéon-Sorbonne.
Vayssière, A., Depret, T., Castanet, C., Gautier, E., Virmoux, C., Carcaud, N., Garnier, A., Brunstein, D., Pinheiro, D., 2016. Etude des paléoméandres holocènes de la plaine alluviale du Cher (site de Bigny, moyenne vallée du Cher). Géomorphologie Relief Process. Environ. 22, 163–176. https://doi.org/10.4000/geomorphologie.11369.
Vinther, B.M., Clausen, H.B., Johnsen, S.J., Rasmussen, S.O., Andersen, K.K., Buchardt, S.L., Dahl-Jensen, D., Seierstad, I.K., Siggaard-Andersen, M.-L., Steffensen, J.P., Svensson, A., Olsen, J., Heinemeier, J., 2006. A synchronized dating of three Greenland ice cores throughout the Holocene. J. Geophys. Res. Atmospheres, 111 https://doi.org/ 10.1029/2005JD006921.
Visset, L., Cyprien, A.L., Carcaud, N., Bernard, J., Ouguerram, A., 2005. Paysage végétal dans le bassin de la Loire moyenne du Tardiglaciaire à l'Actuel. J. Bot. Société Bot. Fr. 29, 41–51.
Voinchet, P., Despriée, J., Gageonnet, R., Bahain, J.-J., Tissoux, H., Falguères, C., Dépont, J., Dolo, J.-M., Courcimault, G., 2007. Datation par ESR de quartz fluviatiles dans le bassin de la Loire moyenne en région Centre: mise en évidence de l'importance de la tectonique quaternaire et de son influence sur la géométrie des systèmes de terrasses. Quaternaire, 335–347 https://doi.org/10.4000/quaternaire.1216.
Wentworth, C.K., 1922. A scale of grade and class terms for clastic sediments. J. Geol. 30, 377–392.
Wintle, A.G., Murray, A.S., 2006. A review of quartz optically stimulated luminescence characteristics and their relevance in single-aliquot regeneration dating protocols.
Radiat. Meas. 41, 369–391. https://doi.org/10.1016/j.radmeas.2005.11.001.